UNCLASSIFIED

| AD NUMBER: | AD0245496 |
| --- | --- |

LIMITATION CHANGES

TO:

Approved for public release; distribution is unlimited.

FROM:

Distribution authorized to US Government Agencies and Contractors only; Administrative/Operational Use; 1 Jun 1960. Other requests shall be referred to Department of Defense, Washington, DC 20301

AUTHORITY

PIB ltr dtd 27 Aug 1970

THIS PAGE IS UNCLASSIFIED

MAPPING OF THE FAR FIELD POLARIZATION
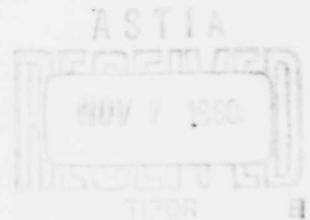OF ANTENNAS BY THE STEREOGRAPHIC PROJECTION

---

THESIS

Submitted in Partial Fulfillment
of the requirements for the
degree of
MASTER OF ELECTRICAL ENGINEERING
at the
POLYTECHNIC INSTITUTE OF BROOKLYN
by
Jerome D. Hanfling

June 1960

61-1-1

**XEROX**

Approved:

_____

_____ 19\_\_

Copy No. \_\_\_\_\_

_____
Head of Department

cry

## VITA

The author was born on ███████ ███ in ████████ ████████ He received his undergraduate education at Brooklyn College and at the City College of New York, and was granted the degree of Bachelor of Electrical Engineering in June 1955 from CCNY. After graduation, and until now, the author has been employed by the Wheeler Laboratories as a development engineer.

The work for this thesis was performed at Wheeler Laboratories during the period 1958-1960.

cry

AN ABSTRACT

MAPPING OF THE FAR FIELD POLARIZATION
OF ANTENNAS BY THE STEREOGRAPHIC PROJECTION

by
Jerome D. Hanfling
Adviser: Dr. J. Blass

Submitted in partial fulfillment of the requirements for
the degree of Master of Electrical Engineering

The purpose of the thesis is to introduce a new method
of mapping of far field polarization of antennas by the stereo-
graphic projection. The mapping of a three dimensional field
plot into a two dimensional one is intended to simplify the
understanding and presentation of antenna polarization.

The far electric field radiation from antennas is
computed in terms of spherical components $\underline{\theta}_o$ and $\underline{\varphi}_o$ and plotted
on an imaginary spherical surface named the radiation sphere.
The spherical components are conformally mapped onto a plane
by the stereographic projection of the radiation sphere. The
plane is constructed to have complex cartesian coordinates
$(w = u + jv)$; the $\underline{u}_o$ direction corresponds to vertical and
the $\underline{v}_o$ direction corresponds to horizontal. On the plane,
the spherical field components are separated into vertical and
horizontal components. The resultant electric field magnitude
and direction at each instant of time over a cycle is then com-
puted and described in terms of elliptical wave polarization
(linear and circular special cases). The wave polarization
properties (axial ratio, tilt angle, sense) are computed by
means of a wave polarization chart, which is a direct analogue
to the Carter admittance chart used in transmission line cal-
culations. By presenting the wave polarization at each point
on the plane, a polarization pattern results.

The polarization patterns of the electric dipole,
magnetic dipole and Huygens source are computed using the

cry

electric current element as a fundamental building block. The linear polarization patterns of the above antennas are families of curves on the plane. The Huygens source is presented as a family of vertical lines and the electric and magnetic dipole as families of circles. Circular polarization patterns are obtained by combinations of the above antennas. The polarization pattern of the turnstile antenna is computed as an example which includes all possible wave polarizations. The results of the computation and presentation of this pattern are extremely interesting and instructive. The polarization loss between two antennas is also analyzed, and given by a general formula.

The method of mapping polarization presented herein is expected to act as a visual aid and analytic tool in the analysis of antenna polarization and in the synthesis of antennas for a specified polarization.

cry

# ACKNOWLEDGEMENTS

cry

# TABLE OF CONTENTS

# TABLE OF FIGURES

cry

# I.   Introduction.

The purpose of the thesis is to introduce a new method of mapping the far field polarization of antennas by the stereographic projection.  This treatment of polarization is expected to aid in the analysis of the antenna far field radiation and in the design of antennas for a specified polarization.  The presentation will describe the stereographic projection as a powerful visual aid and analytic tool which can be used in solving polarization problems and in presenting these solutions.

The thesis will include the following topics: derivation of far electromagnetic field radiation from current elements, discussion of the radiation sphere and polarization, description of the stereographic projection of the radiation sphere, derivation of mapping formulas, computation and mapping of linear, elliptical, and circular polarization patterns of antennas, and analysis of polarization loss between two antennas using projection.

cry

## II.  Electromagnetic Radiation from Current Elements.

Electromagentic radiation is established from dipole moments as a result of the movement of electric charge in elemental lengths.  The radiation is directed outward from the source by time varying electric and magnetic fields.  A general equation for the electric field radiation as a function of the source current can be derived from Maxwell's equations.  From this equation an expression for the near and far fields of a short current element can be obtained.

The fields associated with radiation are formally expressed in terms of rectangular and spherical coordinate systems. These systems are described in Fig. 1.  Point location in rectangular coordinates is determined by x, y, z; vector direction by $\underline{x}_o$, $\underline{y}_o$, $\underline{z}_o$.  Point location is spherical coordinates is determined by r, $\theta$, $\varphi$, vector direction by $\underline{r}_o$, $\underline{\theta}_o$, $\underline{\varphi}_o$.

The general electric field equations for source currents are derived from Maxwell's equations.  Maxwell's equations describe the experimental results of Ampere and Faraday mathematically in a consistent set of equations.  They relate the electric and magnetic fields to the source excitation and are listed below for convenience (Ref. 7).

$$\nabla \times \underline{H} = e\frac{\partial \underline{E}}{\partial t} + \sigma \underline{E} \tag{1}$$

$$\nabla \times \underline{E} = -\mu\frac{\partial \underline{H}}{\partial t} \tag{2}$$

$$\nabla \cdot \underline{B} = 0 \tag{3}$$

$$\nabla \cdot \underline{D} = \rho \tag{4}$$

By solving these equations in terms of source current excitation ($\underline{J}$) and using the concept of vector potential $\underline{A}$ ($\underline{H} = \nabla \times \underline{A}$) it can be shown that:

$$\nabla^2 \underline{A} = \mu e \frac{\partial^2 \underline{A}}{\partial t^2} - \underline{J} \tag{5}$$

cry
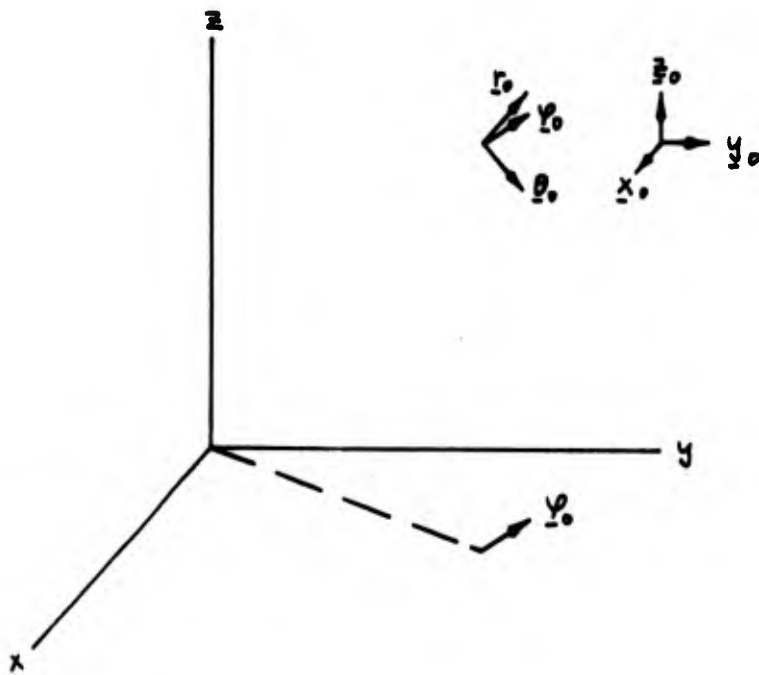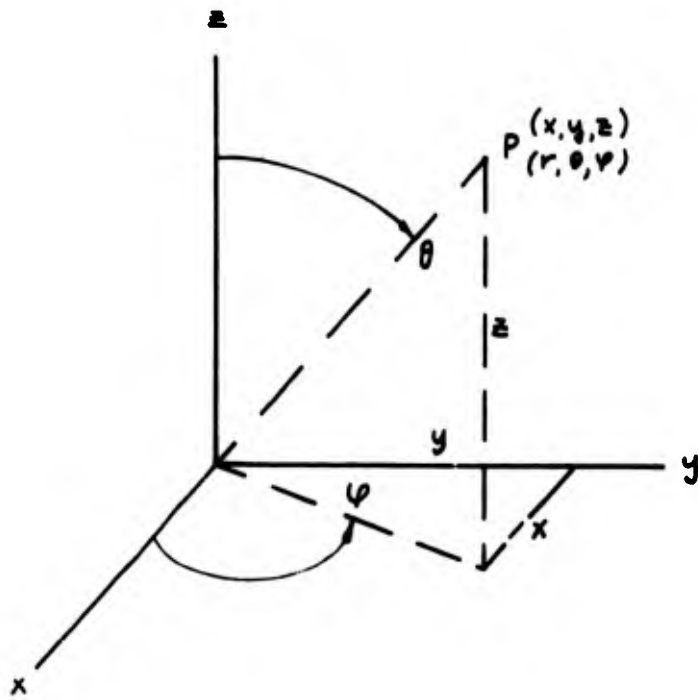
Fig. 1 - Rectangular and spherical coordinate systems.

$$\underline{E} = -J \left( \frac{1}{\epsilon\omega} \nabla\nabla \cdot \underline{A} + \mu\omega\underline{A} \right) \tag{6}$$

This is the general equation for the electric field in terms of the vector potential (Ibid).

The near and far fields of a short current element can be obtained from the above general electric field equation. Assume a dipole moment made up of a length $\Delta l$ pointed in the z direction carrying a current ($I \exp j\omega t$). It can be shown that if $\underline{I}$ is a function of ($wt-\beta r$) and $\underline{A} = \int I\Delta l/4\pi r$ where $\Delta l$ is the differential length of the current element, then equation (5) will be satisified. It is noted that the vector potential will always be in the direction of the current element. Assuming

$$I = |I| \ \exp \ j(\omega t - \beta r) \ \underline{z}_0 \tag{7}$$

$$A = \int \frac{|I| \ \exp \ j(\omega t - \beta r) \ dz \ \underline{z}_0}{4\pi r} \tag{8}$$

If $\Delta l$ approaches a length (a) which is very small compared to $\lambda$ and r then

$$A_z = \frac{Ia \ \exp \ j(\omega t - \beta r)}{4\pi r} \tag{9}$$

the integrand being practically constant over the range of integration. The vector potential in the $\underline{r}_0$, $\underline{\theta}_0$ and $\varphi_0$ directions can then be found from the following:

$$A_r = (\underline{A} \cdot \underline{r}_0)\underline{r}_0 = \frac{|I| a \ \cos \ \theta}{4\pi r} \tag{10}$$

$$A_\theta = (\underline{A} \cdot \underline{\theta}_0)\underline{\theta}_0 = - \frac{|I| a \ \sin \ \theta}{4\pi r} \tag{11}$$

$$A_\varphi = (\underline{A} \cdot \underline{\varphi}_0)\underline{\varphi}_0 = 0 \tag{12}$$

cry

The electric field may be found from equation (6) from which it can be seen that the electric field will be in the same direction as the vector potential. By substituting equations (9) (10) and (11) into ( 6 ):

$$E_r = \frac{Ia \cos \theta}{2\pi r} \left[ \frac{1}{r} \sqrt{\frac{\mu}{\epsilon}} + \frac{1}{j\omega\epsilon r^2} \right] \qquad (13)$$

$$E_\theta = \frac{Ia \sin \theta}{4\pi 4} \left[ j\omega\mu + \frac{1}{r} \sqrt{\frac{\mu}{\epsilon}} + \frac{i}{j\omega\epsilon r^2} \right] \qquad (14)$$

$$E_\varphi = 0 \qquad (15)$$

At considerable distance from the current-carrying wire, r becomes sufficiently large that $\lambda/r$ and its powers are negligible. This means that the electric component $E_r$ drops out rapidly leaving only $E_\theta$ which becomes:

$$E_\theta = \frac{j\omega\mu Ia \sin \theta}{4\pi r} \qquad (16)$$

This result can also be obtained from

$$\underline{E} = -j\omega\mu \left[ (\underline{A} \cdot \underline{\theta}_0) \, \underline{\theta}_0 + (\underline{A} \cdot \underline{\varphi}_0) \underline{\varphi}_0 \right] \qquad (17)$$

where

$$\underline{A} = \frac{Ia}{4\pi r} \qquad (18)$$

and when substituted in equation (17) becomes

$$\underline{E} = -\frac{j\omega\mu a}{4\pi r} \left[ (\underline{I} \cdot \underline{\theta}_0)\underline{\theta}_0 + (\underline{I} \cdot \underline{\varphi}_0) \underline{\varphi}_0 \right] \qquad (19)$$

which holds for the far electric field of a short current element oriented in any direction. The relationships necessary to solve equation (19) are listed below and described in Fig. 2.

$$\underline{I} = a \underline{x}_0 + b \, \underline{y}_0 + c \, \underline{z}_0 \qquad (20)$$

cry
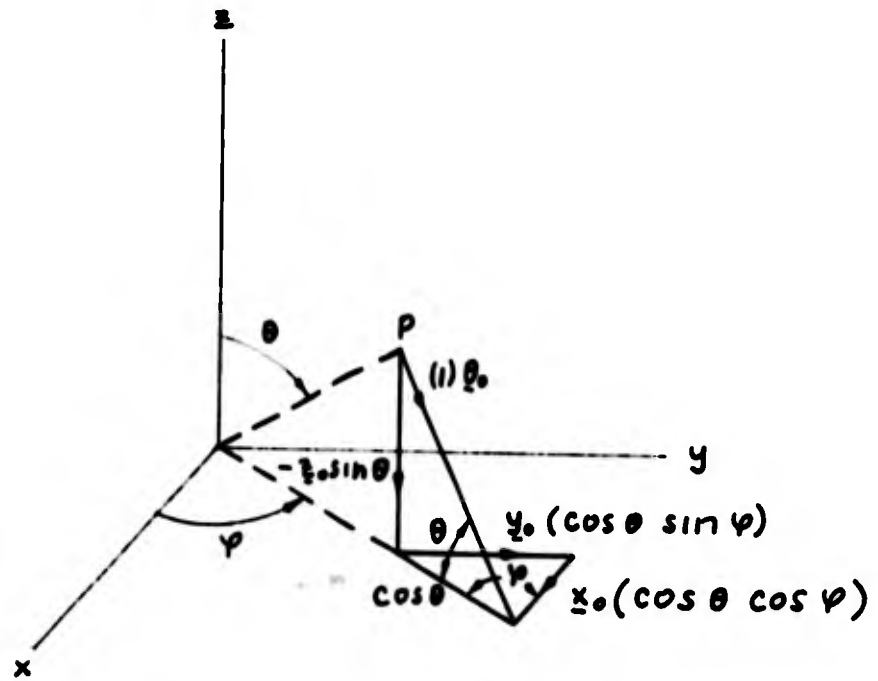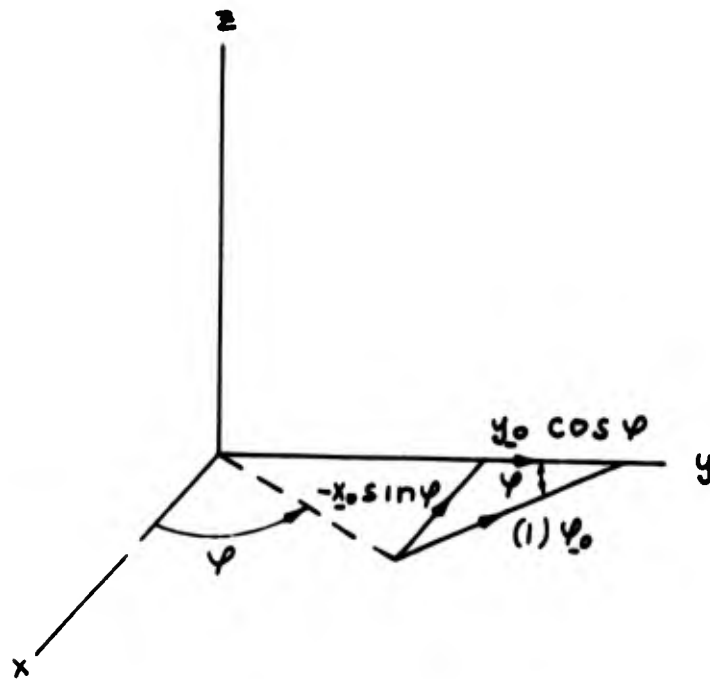
(a) $\quad \underline{\theta}_0 = \cos\theta \, \cos\varphi \, \underline{x}_0 + \cos\theta \, \sin\varphi \, \underline{y}_0 - \sin\theta \, \underline{z}_0$

(b) $\quad \underline{\varphi}_0 = -\sin\varphi \, \underline{x}_0 + \cos\varphi \, \underline{y}_0$

Fig. 2 - Vector transformations.

$$\underline{\theta}_0 = \cos \theta \cos \varphi \; \underline{x}_0 + \cos \theta \sin \varphi \; \underline{y}_0 - \sin \theta \; \underline{z}_0 \qquad (21)$$

$$\underline{\varphi}_0 = -\sin \varphi \; \underline{x}_0 + \cos \varphi \; \underline{y}_0 \qquad (22)$$

Formula (19) for the far electric field will be used for many of the derivations in the remaining portions of the thesis.

cry

### III.  Radiation Sphere and Polarization.

The far electric field radiation from any antenna
can be uniquely described by a gain-polarization pattern.  The gain-
polarization pattern consists of a plot of the wave polarization
and power density normalized to that of an isotrope for each
direction ($\theta, \varphi$ ) from the antenna.  The imaginary spherical sur-
face centered on the antenna, and upon which the fields are
plotted, is so useful that it has been named the radiation
sphere.  The radiation sphere, wave polarization, and polari-
zation pattern are discussed below.  The methods of computing
the wave polarization ellipse are also described.

For convenience, the radiation sphere is chosen to
have a diameter of unity as shown in Fig. 3.  The sphere
derives its usefulness from the properties of the far field.
First the electric field is perpendicular to the radius vector
($r_o$) and can be represented by a small line segment tangent
to sphere, second the gain (power density normalized to an
isotrope) is only a function of $\theta$ and $\varphi$ and is the same for
all spheres concentric with the antenna, and lastly the
direction ($\theta, \varphi$) can be represented by a point on the sphere.

The wave polarization is defined as the magnitude and
direction of the electric field at each instant of time over
a cycle for a specific point on the radiation sphere.  The
wave polarization is, in general, elliptical, but linear, a
degenerate form and circular are usually considered as special
cases.  When the wave polarization of every point on the
radiation sphere is considered, the resultant field plot is
called a polarization pattern.  In general, the polarization
pattern will be elliptical, but for certain antennas can be
separated into linear and circular.  When the gain is also
included, the field plot will be called a gain-polarization
pattern.

For linear wave polarization the magnitude of the
electric field vector varies sinusoidally from positive to
negative values over a cycle while the reference direction
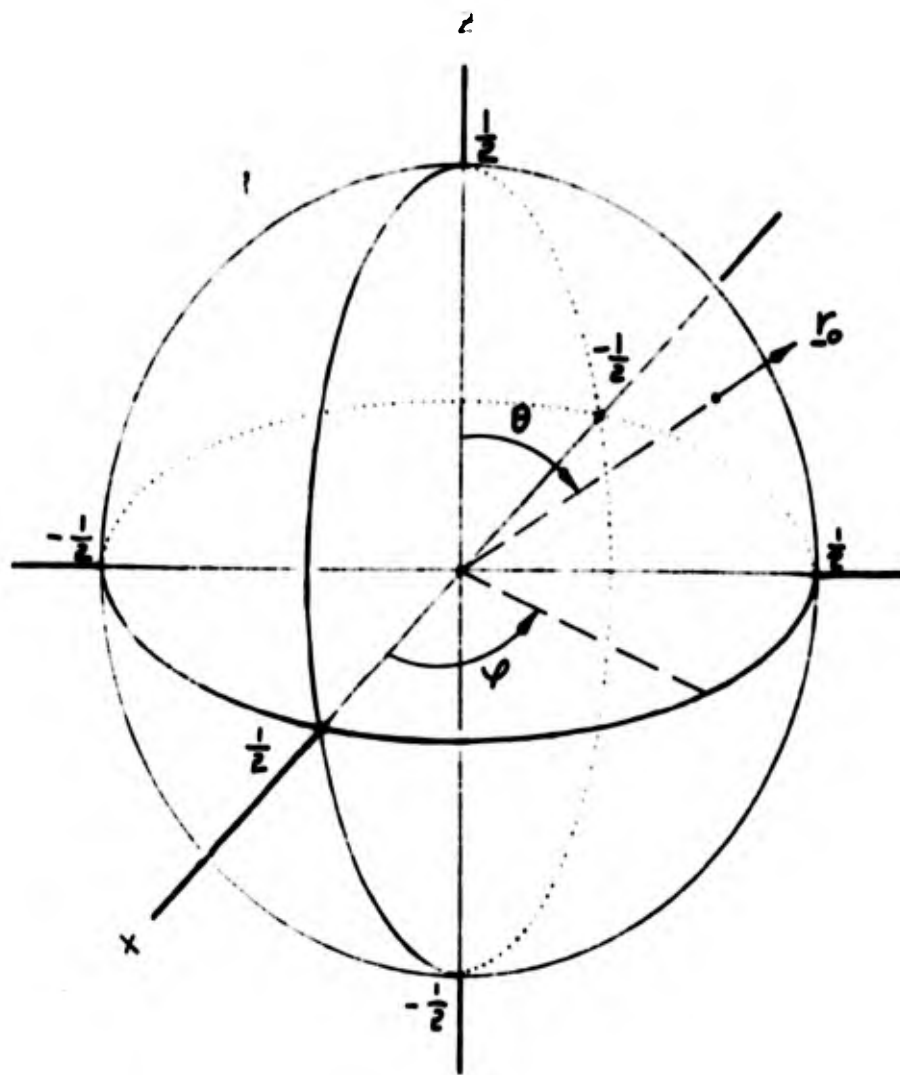remains fixed, as shown in Fig. 4(a) (Ref. 10).  A linear
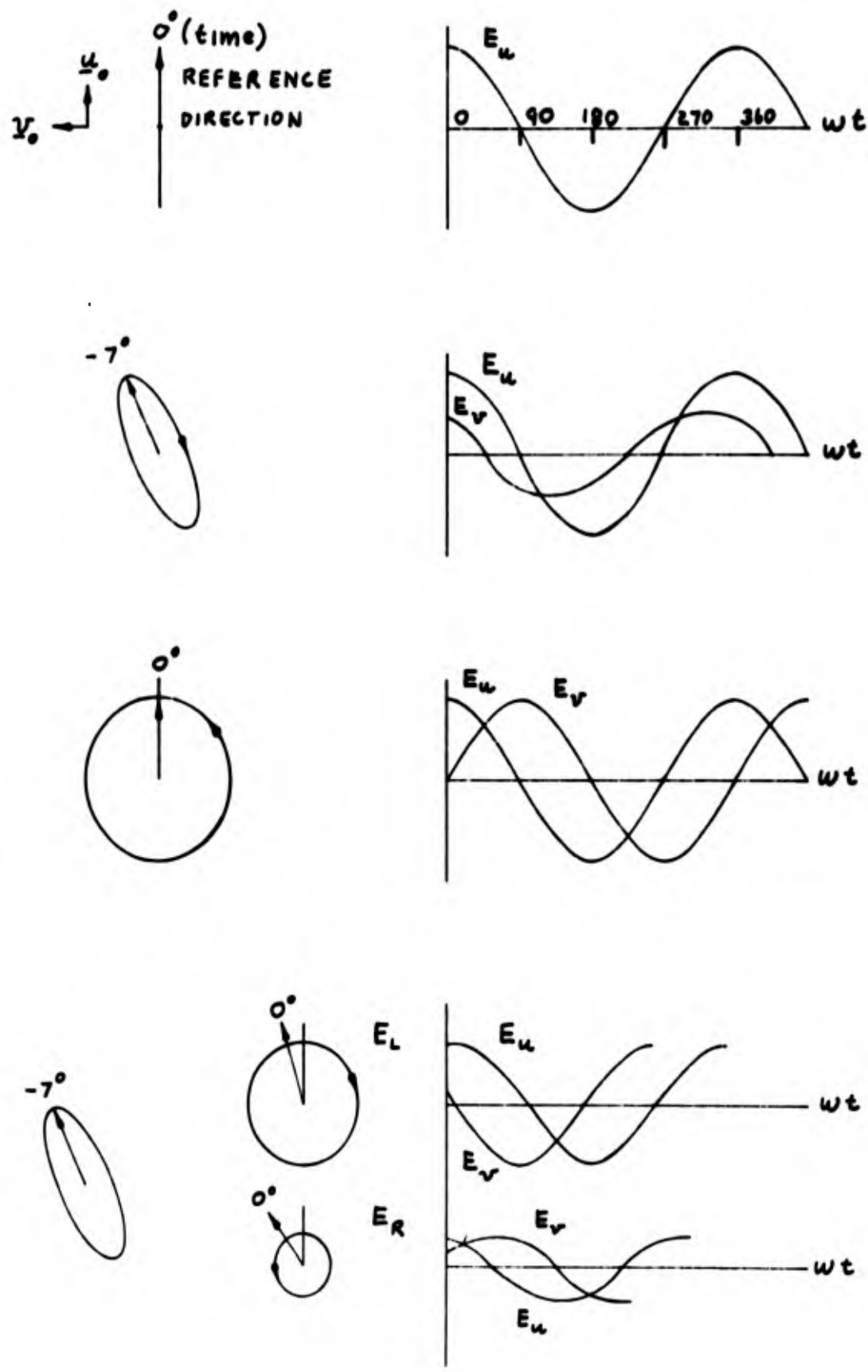
cry

Fig. 3 - The Radiation Sphere.

Fig. 4 - Wave polarization.

polarization pattern will occur when the wave polarization is
linear for each location on the radiation sphere. This results
in a family of curves (loci) on the surface of the sphere.

For elliptical wave polarization the magnitude and
direction of the electric field vector vary with time, as shown
in Fig. 4(b). The tip of the E-vector rotates clockwise or
counterclockwise (from some reference direction) describing
an ellipse each cycle; the direction of rotation is called the
sense (ibid). The convention to be used here is shown in Fig. 5
for an approaching wave. When the major and minor axes of the
ellipse are equal, the wave polarization is called circular,
Fig. 4(c). When the wave polarization is circular for all
points then a circular polarization pattern results.

The wave polarization ellipse can be uniquely described
in terms of the axial ratio, tilt angle, and sense. These
quantities are shown in Fig. 5 for an approaching wave; they
are referenced to an u, v, coordinate system which will be
described in detail in Section IV. In order to compute the
quantities listed, the wave polarization ellipse can be
thought of as produced by two linearly polarized waves of the
same frequency or two circularly polarized waves also of the
same frequency (Ref. 8). The two linearly polarized waves are
of arbitrary amplitude and time phase, but are orthogonal in
space as shown in Fig. 4(b). The two circularly polarized
waves are of arbitrary amplitude, of opposite sense and in
time phase in the direction of the major axis of the resulting
ellipse, as shown in Fig. 4(d). In this thesis, both concepts
will be used to compute the polarization ellipse.

The method to be used herein for computation of the
polarization ellipse is based on the analogy between the
orthogonal transverse electric fields in polarization and the
orthogonal transverse electric and magnetic fields in trans-
mission lines (Ref. 11, 13). In computing the polarization
ellipse the magnitude and phase of the ratio of the linearly
polarized wave amplitudes is seen to be analogous to the
magnitude and phase of normalized admittance; the ratio of the
left to the right circularly polarized waves is analogous to

cry

the ratio of reflected to incident waves (reflection coefficient) and the tilt angle to the phase of reflection coefficient; the axial ratio term is taken to be analogous to the standing wave ratio. An example (referenced to the u, v, coordinates shown in Fig. 5) is given to demonstrate the above view point, the formulas used are derived in Appendix I.

The transverse wave amplitude $|E_u|$ and $|E_v|$ and time phase are given.

$$E_u = 0.4 - j0.1 = 0.5 \; \underline{/-36.8^o} \tag{23}$$

$$E_v = -0.3 + j0.85 = 0.9 \; \underline{/103.4^o} \tag{24}$$

The corresponding amplitude ratio $|P|$ and phase difference ($\delta$) are

$$P = |P| \; \underline{/\delta} = \frac{E_v}{E_u} = 1.8 \; \underline{/146.2^o} \tag{25}$$

$$P = -1.5 + j1 \tag{26}$$

P is modified by j to make the analogy to admittance consistent, see Appendix I.

$$jP = p = -1 - j1.5 \tag{27}$$

In order to find the axial ratio, tilt angle, and sense, the ratio between the left and right circularly polarized components (q) is found, just as the reflection coefficient is needed to compute the SWR and phase. For q less than 1 the sense is right-handed or counterclockwise. If q is greater than 1 the sense is left-handed or clockwise and $q' = \frac{1}{q}$ must be substituted in the analysis.

$$q = \frac{L}{R} = \frac{1-p}{1+p} = \frac{2 + j1.5}{-j1.5} = 1.66 \; \underline{/126.8^o} \tag{28}$$
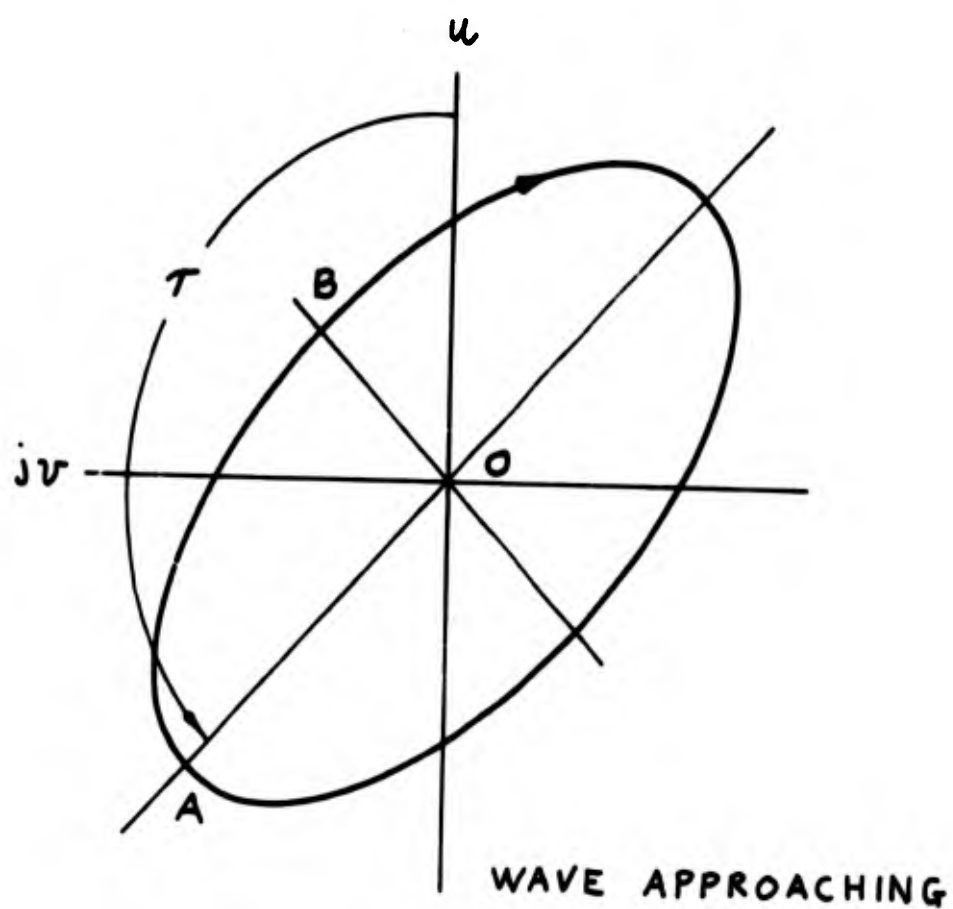
$$q' = \frac{1}{1.66} \; \underline{/-121.8^o} = 0.6 \; \underline{/-126.8^o} \tag{29}$$

cry

Fig. 5 - Wave polarization ellipse.

$$P = |P| \angle \delta = \frac{E_v}{E_u}$$
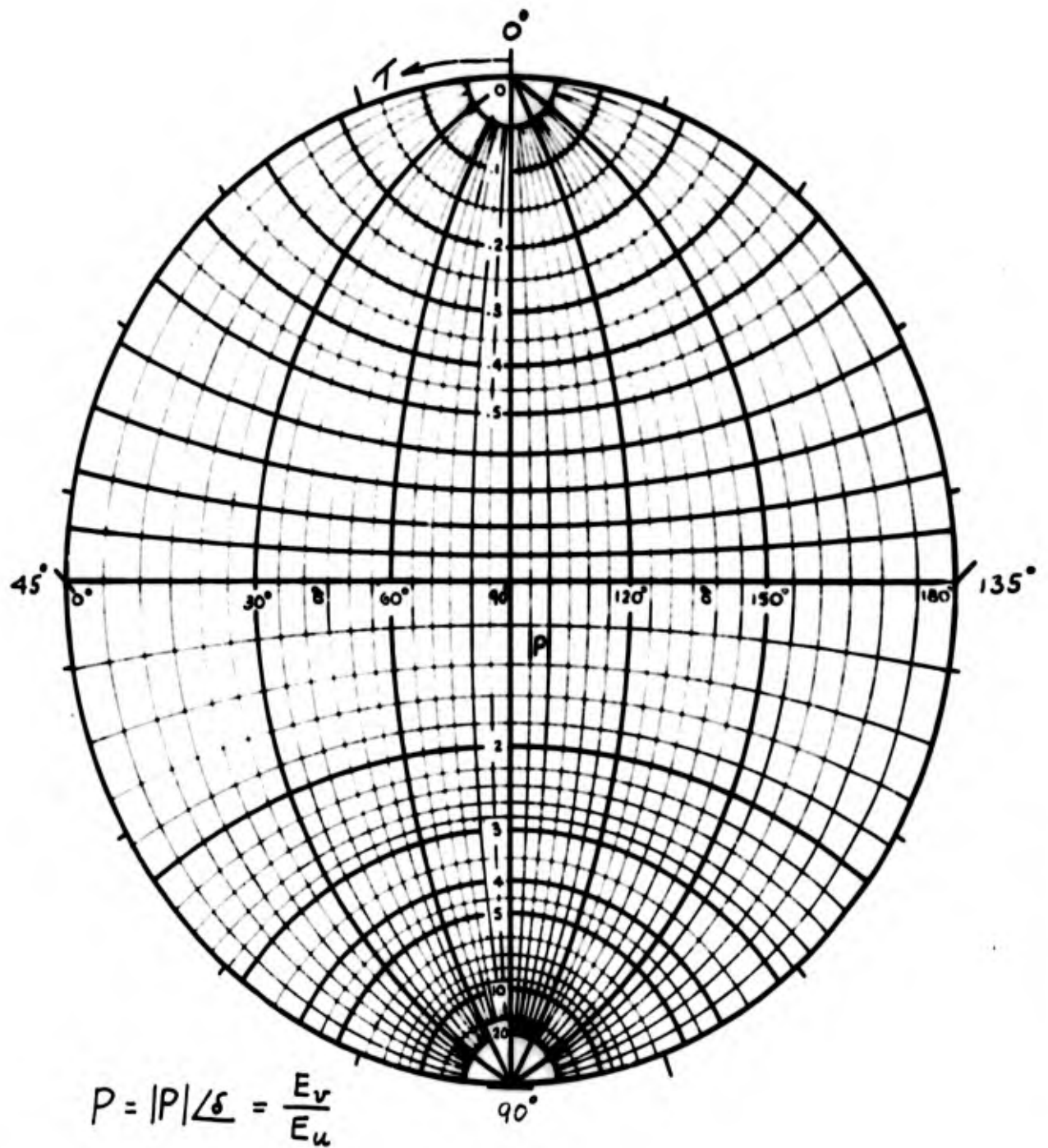
Fig. 6 - Wave polarization chart.

$$q' = |q'| \exp -j2\tau \tag{30}$$

From the magnitude of (q') the axial ratio may be computed

$$r = \frac{1 + |q'|}{1 - |q'|} = \frac{1 + 0.6}{1 - 0.6} = 4 \tag{31}$$

From the phase of q' the tilt angle ($\tau$) is computed.

$$\tau = \frac{1}{2}(-126.9^{\circ}) = -63.4^{\circ} \text{ or } 116.6^{\circ} \tag{32}$$

Rather than have to analytically compute the polarization ellipse each time, a wave polarization chart similar to the Carter impedance chart has been developed by Deschamp and Rumsey (Ref. 11 and 15). This chart is shown in Fig. 6. The small circles are lines of constant $|P|$ while the great circles are lines of constant ($\zeta$). The above example has been carried out on the chart shown.

In Kraus (Ref. 10) formulas are developed in terms of the linearly polarized components of the wave independent of the transmission line analogy. As a check, the above example has also computed from these formulas.

The example given in this section has been taken from the polarization pattern computation of the turnstile antenna (Section VII) for $\theta = \varphi = 30^{\circ}$.

## IV.  Stereographic Projection of the Radiation Sphere.

The stereographic projection of the radiation sphere is used to map the antenna polarization pattern from the radiation sphere to a complex plane.  By mapping the three dimensional field plot into a two dimensional field plot the analysis, computation, visualization and general understanding of antenna polarization is greatly simplified.  The discussion that follows includes a description of the stereographic projection, and complex plane, and a derivation of formulas for the transformation of locations and directions from spherical coordinates to complex plane coordinates.

The stereographic projection is a geometrical construction associating every point on a sphere (except pole $\theta = \varphi = 0^{0}$) with a unique point on a plane; for the analysis the plane is taken to be complex.  The construction of the projection is shown pictorially in Fig. 7 (Ref. 2 and 18).  The radiation sphere surrounds the antenna and is tangent to the plane at point (0).  The points on the sphere are transformed to the plane by straight lines from pole 0' through the sphere to the plane.  The projection is conformal, meaning that the magnitude and sense of angular relationships between intersecting curves on sphere and the corresponding ones on the plane are preserved; the infinitesimal shapes of areas about any one point of the sphere are preserved although they may be magnified or shrunk (Ref. 6).  The projection transforms circles on the sphere to circles on the plane (straight line special case of circle); in particular, circles on the sphere which pass through pole 0' become straight lines on the plane.  The polarization pattern for the entire sphere may be mapped on the plane as a result of the properties of the stereographic projection.  An interesting mathematical proof of the conformal properties of the stereographic projection can be found in (Ref. 1).

The mapping of antenna polarization is accomplished analytically by the introduction of a complex plane, using Cartesian coordinates as shown in Figs. 7 and 8 (Ref. 5).  This
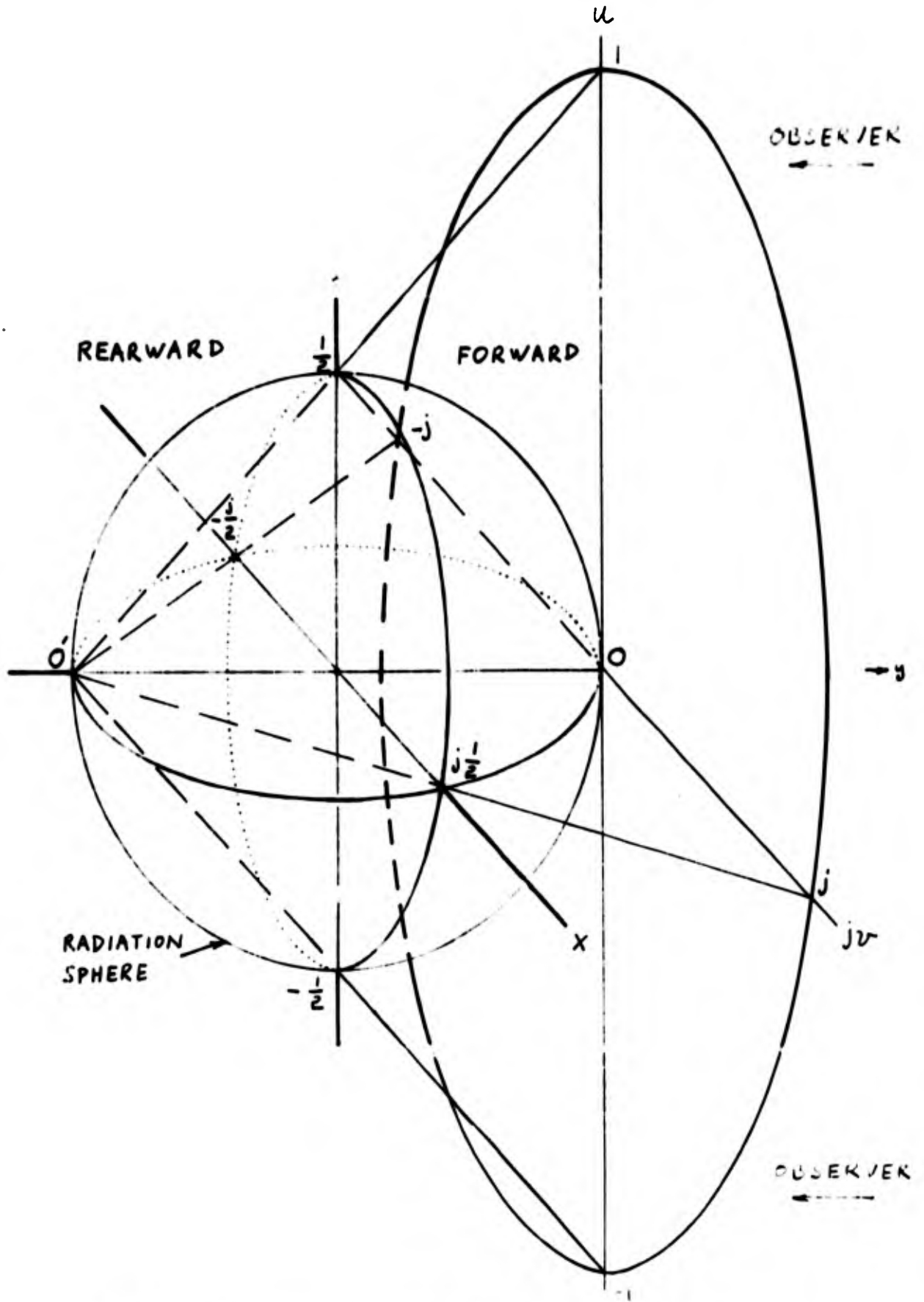
cry

Fig. 7 - Stereographic projection of radiation sphere.

has been done to simplify computations and to reference all polarizations to a fixed direction, namely vertical polarization. The real axis (u) is chosen as vertical pointing toward the top of the page and the imaginary axis (v) is horizontal pointing toward the left, which is equivalent to the standard complex plane rotated counterclockwise by $90^\circ$.

The projection of the u and v axes to the plane from the radiation sphere is represented pictorially in Fig. 7 (Ref. 12). The great circle 0, $-j\frac{1}{2}$, 0, $j\frac{1}{2}$ projects into the v axis, the great circle 0, $-\frac{1}{2}$, 0', $\frac{1}{2}$ projects into the u axis and the great circle $-\frac{1}{2}$, $-j\frac{1}{2}$, $+\frac{1}{2}$, $+j\frac{1}{2}$ projects into a circle of unit radius. All of the projected points within this circle are in the forward hemisphere and all the points outside the circle are in the rearward hemisphere. For convenient representation in this thesis, the polarization pattern will be mapped within the unit circle for one hemisphere at a time.

The correspondence between points and vectors on the sphere and plane is shown in Fig. 8, by an end-view of the radiation sphere and a projected side-view of the forward hemisphere. Any point in the plane is defined by $w = u + j\,v$ and is located at the intersection of straight lines parallel to the coordinate axes. The corresponding point on the sphere is located at the point (P) which is the intersection of orthogonal circles containing the point (P) and perpendicular to the coordinate planes. Any vector at a point in the complex plane is defined by components in the $\underline{u}_0$ and $\underline{v}_0$ directions. The corresponding vector on the sphere has components tangent to the two orthogonal circles at this point.

The intention of this thesis is to map the polarization vectors on the complex plane by computing their components in the $\underline{u}_0$ and $\underline{v}_0$ directions. When every vector at every point is mapped in this manner, a complete two dimensional representation of the polarization pattern in Cartesian coordinates is obtained.(the polarization pattern for each hemisphere is inside a circle of unit radius). It must be pointed out at this time that initially the polarization vectors could have been analyzed by $\underline{\theta}_0$ and $\underline{\varphi}_0$ components on the plane rather than
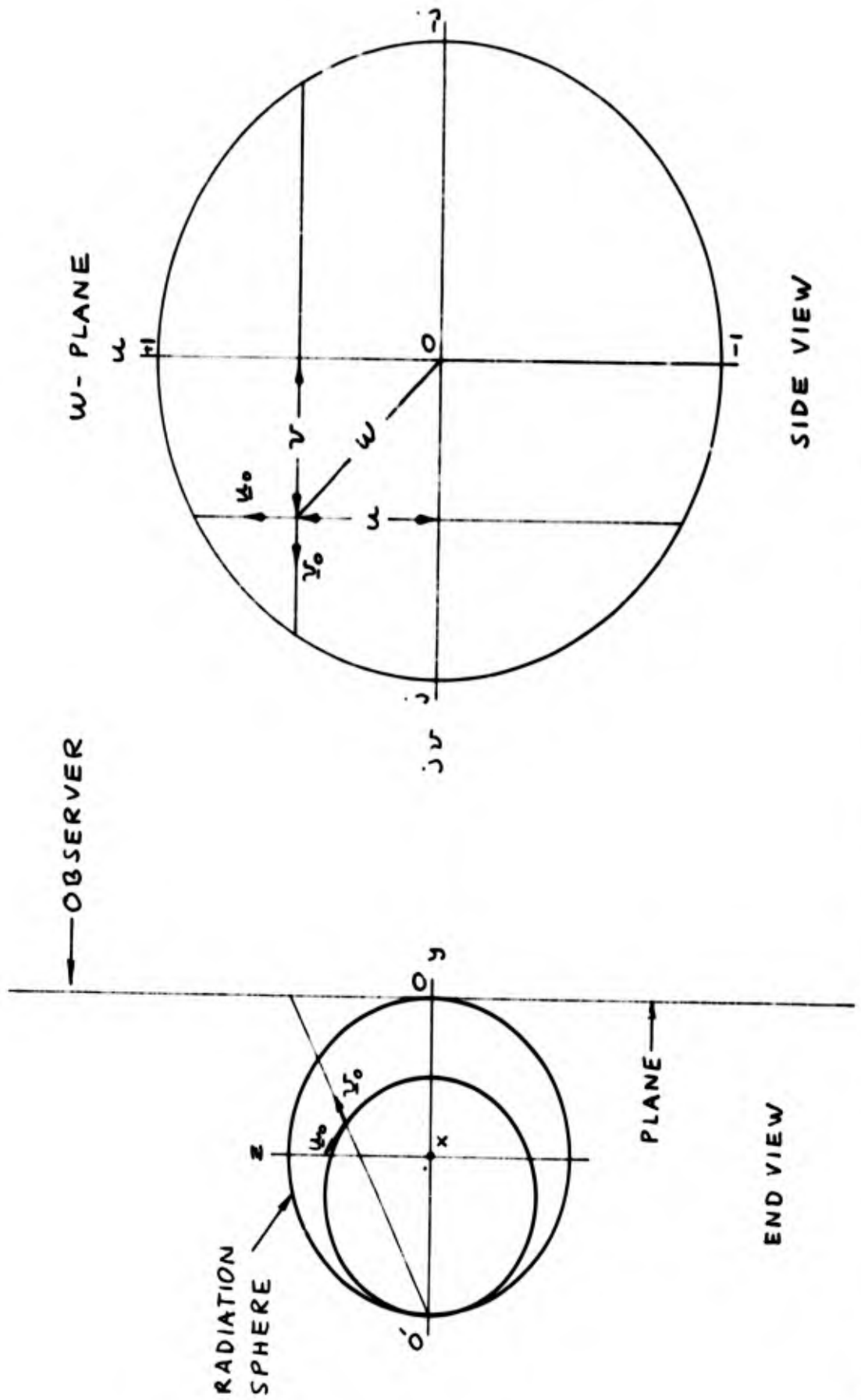
Fig. 8 - Construction of complex plane coordinates and directions.

separating them into $\underline{u}_o$ and $\underline{v}_o$ components. Two among the advantages of the latter, are that there exists a fixed direction to which the resultant elliptical and linear wave polarizations could be referred and that it is sometimes convenient to compute the general equation and form of linear polarization loci and elliptical polarization patterns (Section VII).

The polarization of the antenna and directional from the antenna has been computed in Section II in terms of spherical coordinates. The location of a point on the sphere being given by $\theta$ and $\varphi$, and direction of the polarization vector by components in the $\underline{\theta}_o$ and $\underline{\varphi}_o$ directions. The point location and vector directions are transformed to the plane by a series of trigonometrical and geometrical transformations.

The location of point P on the sphere is given in Fig. 9 in terms of $(90 - \varphi)$ (angle between great circles A and B) and $\varphi$ (angle between z axis and small circle D). An alternate · representation, which is helpful in computation, is also shown in terms of $\beta$ (angle between great circles C and B) and $\chi$ (angle between y axis and small circle E). The formulas relating the two conventions are listed below and in Fig. 5.

$$\sin \chi = \frac{\cos \theta}{\cos \beta} \tag{33}$$

$$\cos \chi = \sin \theta \sin \varphi \tag{34}$$

$$\tan \frac{\chi}{2} = \frac{\sin \chi}{1 + \cos \chi} \tag{35}$$

The stereographic projection of any point P $(\theta, \varphi)$ on the sphere to a corresponding point P $(u, v,)$ on the plane is derived from Fig. 10 using the same end view representation as in Fig. 8 (Ref. 12). Each point can also be considered to have coordinates $\beta$ and $\chi$ in order to simplify the derivation. The points are located at an angle $\beta$ with respect to the u axis and at a length $\tan \chi /2$ from the origin O. The u, v components of the points are

$$u = \tan \frac{\chi}{2} \cos \beta \tag{36}$$

cry
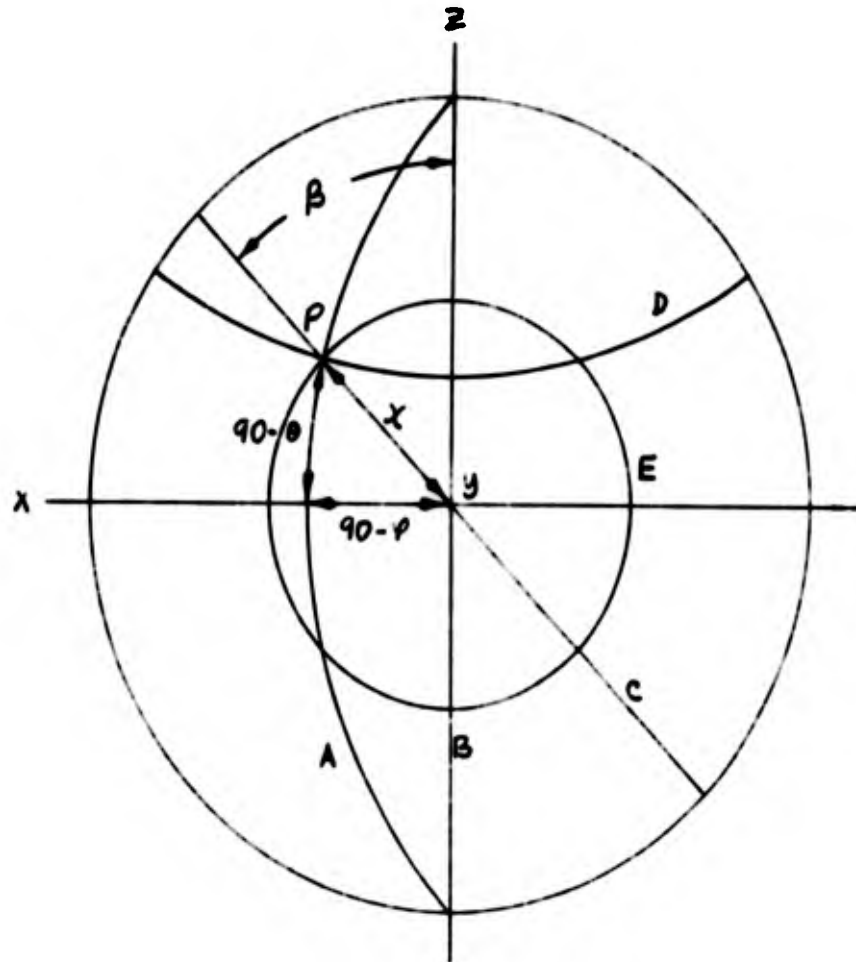
$$\sin x = \cos \theta / \cos \beta$$

$$\cos x = \sin \theta \sin \varphi$$

$$\tan x/2 = \sin x / 1 + \cos x$$

Fig. 9 - Trigonometry of polar and meridional components on representation of sphere.

$$v = \tan \frac{x}{2} \sin \beta \tag{37}$$

By substituting the trigonometric relationships (33) (34) and (35) into equations (36) and (37) u and v can be expressed as a function of $\theta$ and $\varphi$.

$$u = \frac{\cos \theta}{1 + \sin \varphi \sin \theta} \tag{38}$$

$$v = \frac{\sin \theta \cos \varphi}{1 + \sin \varphi \sin \theta} \tag{39}$$

The transformation of vector components in the $\underline{\theta}_0$ and $\underline{\varphi}_0$ directions on the sphere to vector components in the $\underline{u}_0$ and $\underline{v}_0$ directions on the plane is derived in Figs. 11 and 12. In Fig. 11 the great circle and small circle which defines $\underline{\theta}_0$ and $\underline{\varphi}_0$ are mapped conformally on to the plane. The location on the plane of the centers and radii of the circles as a function of $\theta$ and $\varphi$ are derived from Fig. 11. Any point P can be selected with vectors of magnitude A in the $\underline{\theta}_0$ direction and B in the $\underline{\varphi}_0$ direction. The $\underline{\theta}_0$ vector is tangent to the great circle at P and the $\underline{\varphi}_0$ vector is tangent to the small circle at P, as shown in Fig. 12. The angle between the $\underline{\theta}_0$ vector and the $\underline{u}_0$ direction and the angle between the $\underline{\varphi}_0$ vector and $\underline{v}_0$ direction are both equal to $\sigma$. Multiplication of the vector magnitude by $\sin \sigma$ and $\cos \sigma$ will give the $\underline{u}_0$ and $\underline{v}_0$ components as is derived below:

$$E_\theta = A \, \underline{\theta}_0 \; ; \quad E_\varphi = B \, \underline{\varphi}_0 \tag{40}$$

$$E_\theta = -A \cos \sigma \, \underline{u}_0 + A \sin \sigma \, \underline{v}_0 \tag{41}$$

$$E_\varphi = -B \sin \sigma \, \underline{u}_0 - B \cos \sigma \, \underline{v}_0 \tag{42}$$

$$E_u = -A \cos \sigma - B \sin \sigma \tag{43}$$

$$E_v = A \sin \sigma - B \cos \sigma \tag{44}$$

cry

$u = \tan x/2 \; \cos \beta$

$v = \tan x/2 \; \sin \beta$
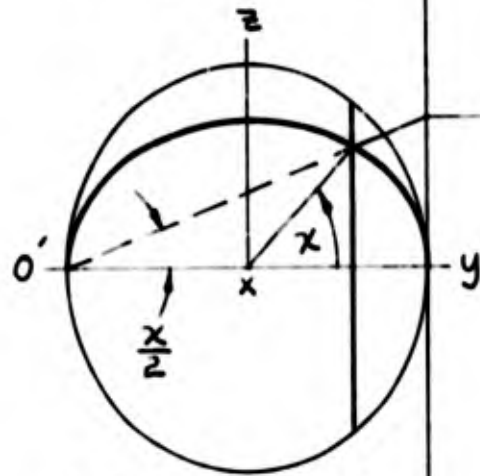
RADIATION SPHERE
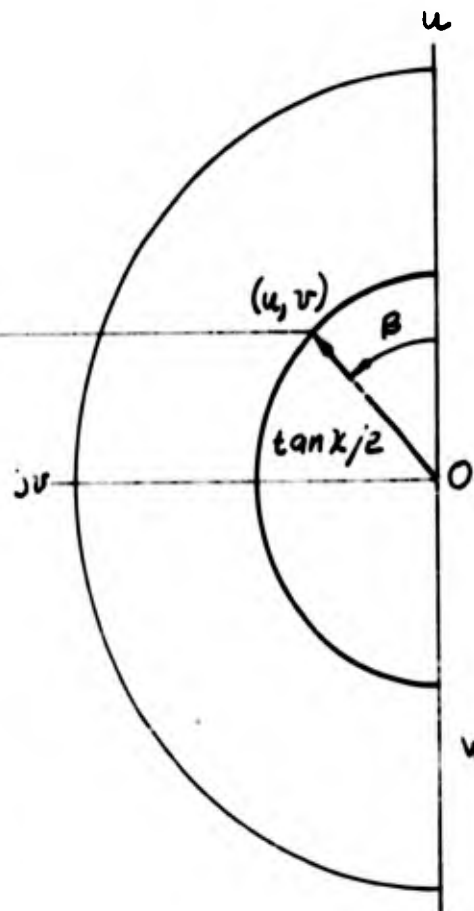
END VIEW

W-PLANE

$u = \cos \theta / 1 + \sin \theta \, \sin \varphi$

$v = \dfrac{\sin \theta \; \cos \varphi}{1 + \sin \theta \; \sin \varphi}$
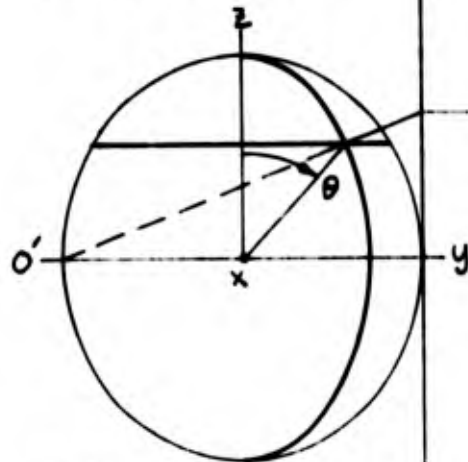
RADIATION SPHERE

END VIEW
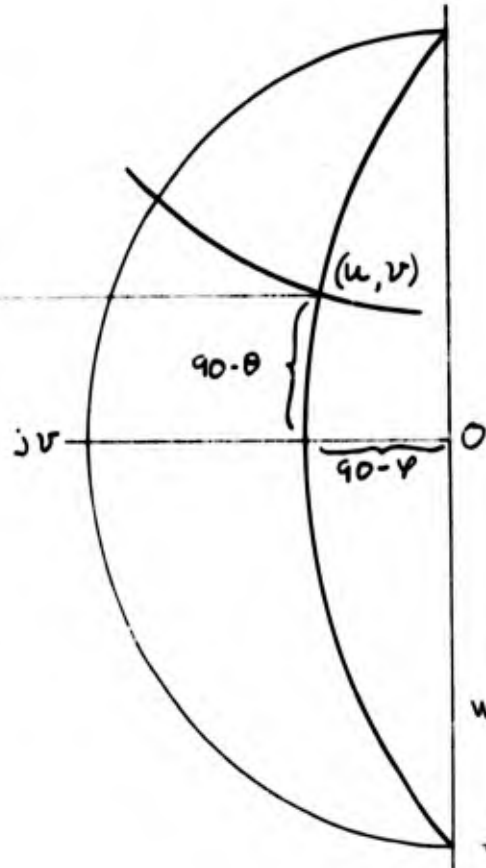
W-PLANE

Fig. 10 - Complex plane point locations from polar and meridional components.

$$u_e = \frac{\cos\theta}{1+\sin\theta}$$

$$u_c = \frac{1}{\cos\theta}$$

$$\rho_\varphi = \tan\theta$$

W-PLANE

$$v_e = \frac{\cos\varphi}{1+\sin\varphi}$$

$$v_c = \tan\varphi$$

$$\rho_\theta = \frac{1}{\cos\varphi}$$
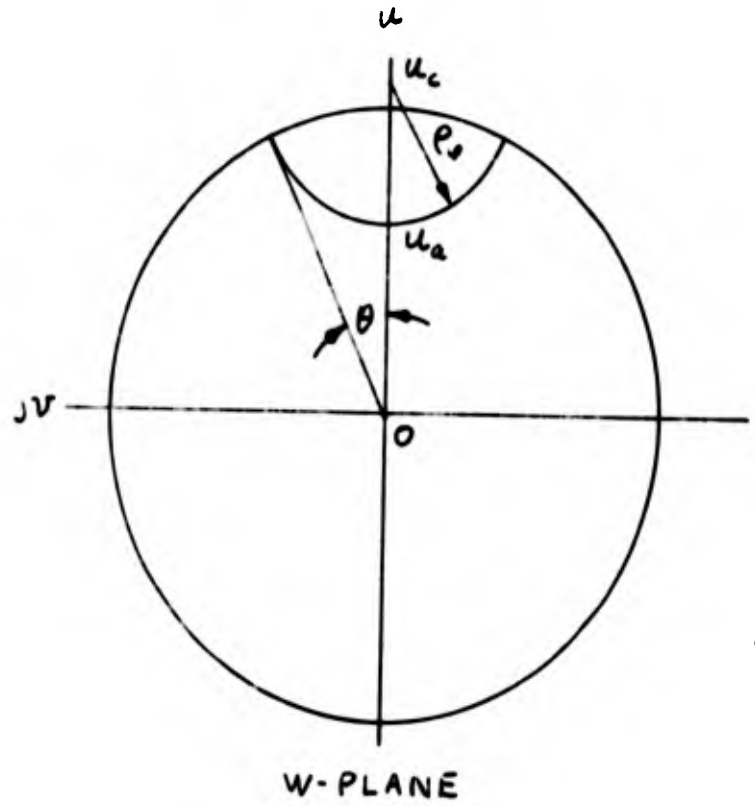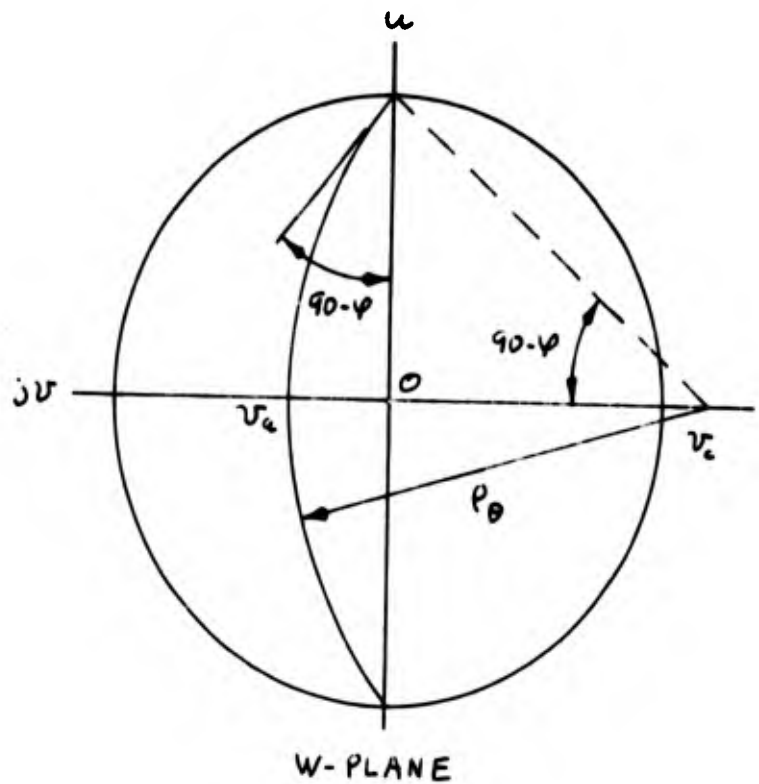
W-PLANE

Fig. 11 - Stereographic projection of small and great circles.

W- PLANE
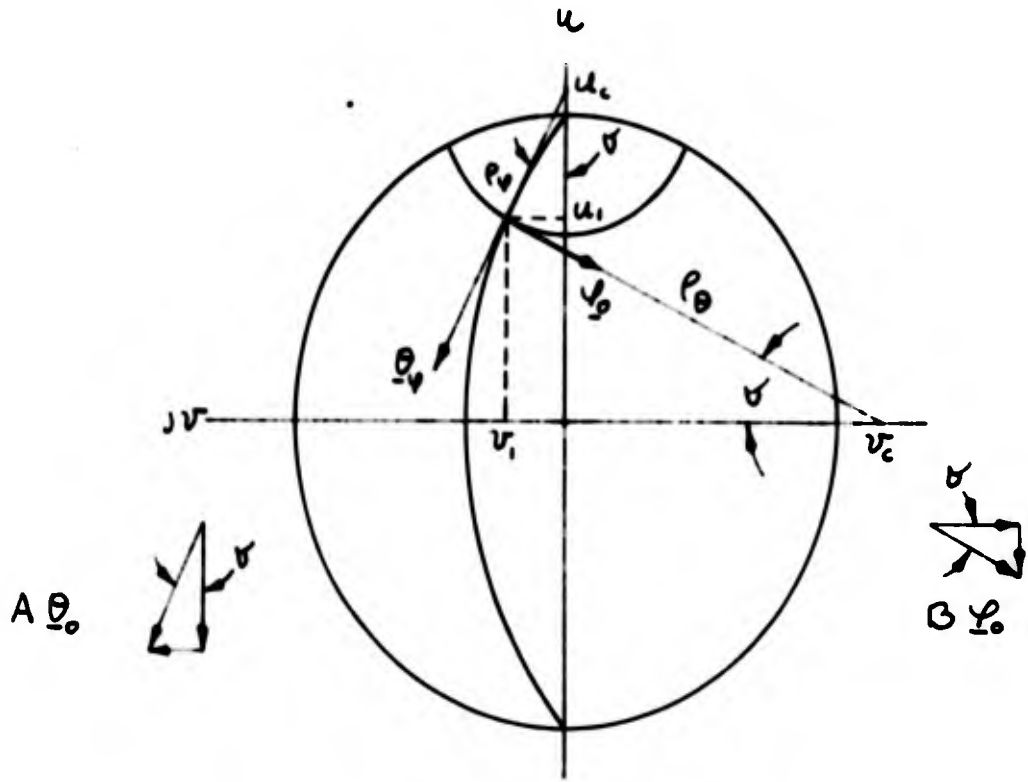
$$\sin \delta = \frac{u_1}{\rho_\theta} = \frac{v_1}{\rho_\varphi} = \frac{\cos \theta \cos \varphi}{1 + \sin \theta \sin \varphi}$$

$$\cos \delta = \frac{v_c + v_1}{\rho_\theta} = \frac{u_c - u_1}{\rho_\varphi} = \frac{\sin \theta + \sin \varphi}{1 + \sin \theta \sin \varphi}$$

Fig. 12 - Transformation of vectors in the $\underline{\theta}_0$ and $\underline{\varphi}_0$ directions to vectors in the $\underline{u}_0$ and $\underline{v}_0$ directions.

$$P = \frac{E_v}{E_u} = \frac{(1 - \frac{A}{B} \tan \sigma)}{(\frac{A}{B} + \tan \sigma)} \tag{45}$$

The relations for the sin σ and cos σ are derived from geometry of Fig. 12 in order to obtain $E_u$ and $E_v$ in terms of θ and φ.

$$\sin \sigma = \frac{\cos \theta \cos \varphi}{1 + \sin \theta \sin \varphi} \tag{46}$$

$$\cos \sigma = \frac{\sin \theta + \sin \varphi}{1 + \sin \theta \sin \varphi} \tag{47}$$

$$\tan \sigma = \frac{\cos \theta \cos \varphi}{\sin \theta + \sin \varphi} \tag{48}$$

From the above equations the wave polarization can be broken up into $E_u$ and $E_v$ components for all points on the sphere. From these vectors the polarization pattern may be computed and mapped with reference to a fixed direction $(\underline{u}_o)$.

cry

## V.  Mapping of Linear Polarization Patterns of Antennas.

The linear polarization patterns of such fundamental radiators as the electric dipole, magnetic dipole and Huygens source are analyzed.  These radiators will be constructed from the electric dipole (short current element) which will be taken as a fundamental building block of all antennas considered in the thesis.  The polarization patterns have been computed and mapped on the complex plane using equations (46) and (47) when necessary.

The electric dipole is taken as a short current element at the origin of the x, y, z coordinate system.  The equation for the far electric field when the element is oriented in the z direction was derived previously and is given below in equation (49).  The far electric field is in the $\theta_0$ direction which is along the meridians or great circles.  The polarization pattern for the forward hemisphere has been plotted on the complex plane as shown in Fig. 13 (a); the arrows designate the reference direction.  The gain could also have been plotted by a series of vectors of varying length along the $\theta_0$ direction or by contours of constant gain (small circles).

When the dipole is oriented in the x direction, the pattern of Fig. 13(a) would be rotated by $90^0$ keeping the u, v axes fixed.  The electric field for this case can be derived from equation (19).  Intuitively, it is known that the polarization pattern on the sphere is invariant; it is solely determined by the type of antenna.  When the dipole is oriented in the y direction, the pattern will be that of Fig. 13(b). Although the answers to case (b) could be derived intuitively, an analysis was performed to check the derivations of the pervious sections.  The far electric field is given below in terms of spherical coordinates.  The electric field was transformed to the complex plane using equations (46) and (47).  The result was the same as Fig. 13(b),  therefore substantiating the method of mapping polarization.

Electric Dipole:

$$_z E = \frac{j\omega\mu Ia \sin\theta \ \theta_0}{4\pi r}$$

(49)

cry
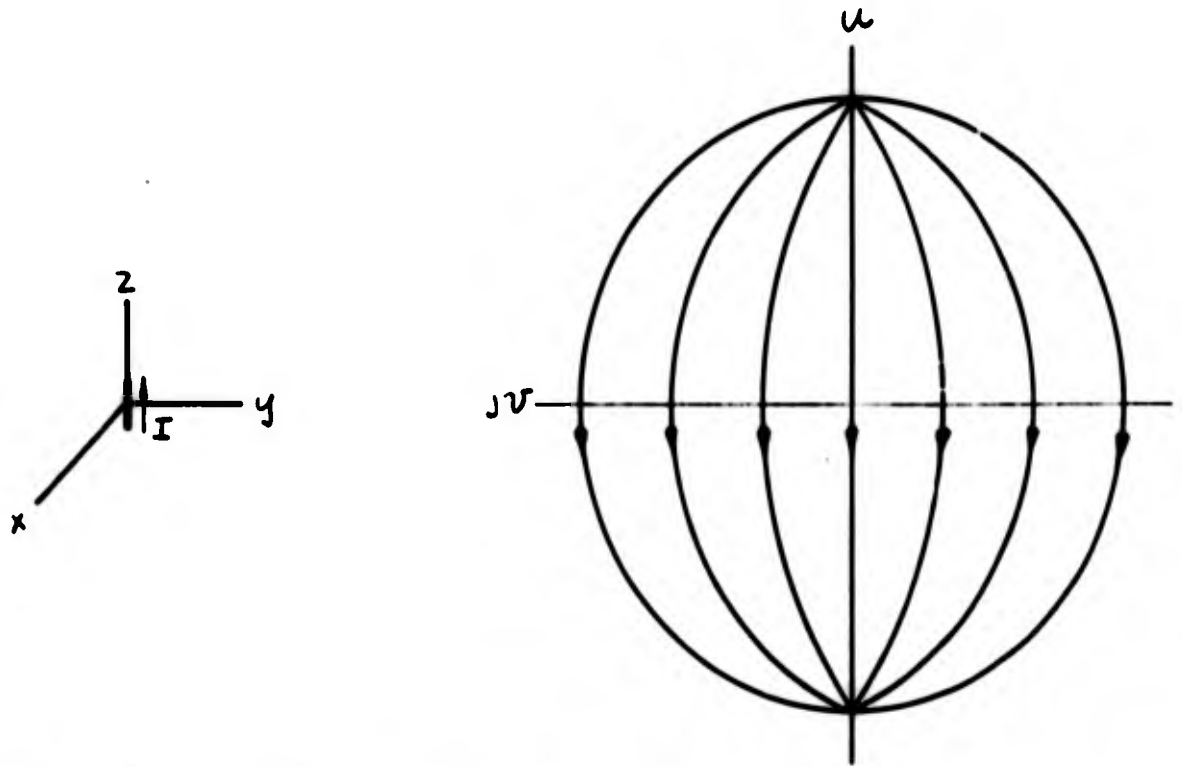
**(a)** Electric dipole - z direction.
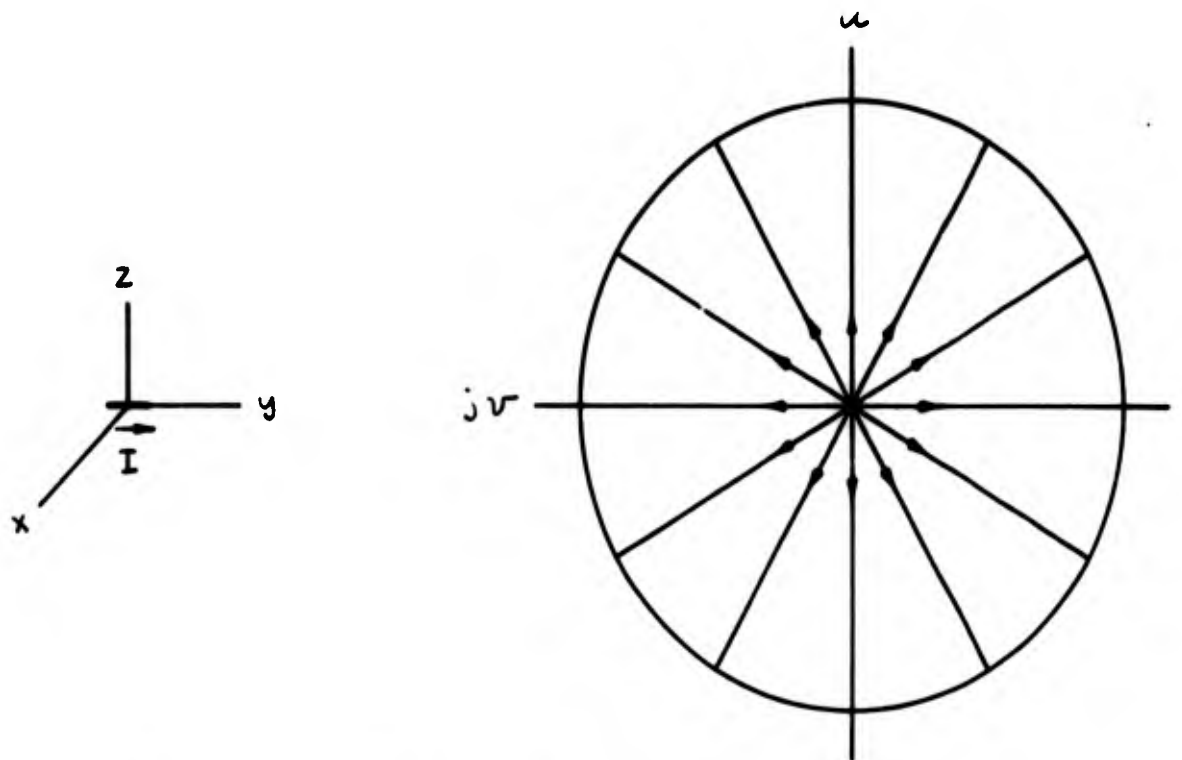


(b) Electric dipole - y direction.

Fig. 13 - Linear polarization patterns of electric dipole.

$$_x E = \frac{-j\omega\mu Ia \ (\cos\theta\cos\varphi \ \underline{\theta}_0 \ - \ \sin\varphi \ \underline{\varphi}_0)}{4\pi r} \tag{50}$$

$$_y E = \frac{-j\omega\mu Ia \ (\cos\theta\sin\varphi \ \underline{\theta}_0 \ + \ \cos\varphi \ \underline{\varphi}_0)}{4\pi r} \tag{51}$$

The second fundamental antenna is the magnetic dipole. This dipole is usually thought of as a small circular loop of wire; here it will be taken as a square loop made up of four electric dipole current elements. For a loop whose axis is oriented in the $\underline{z}_0$ direction, the far electric field is derived in Appendix II and is given below, formula (52). The electric field is in the $\underline{\varphi}_0$ direction for all points on the sphere. The polarization pattern is mapped in Fig. 14(a) showing the electric field along the small circles. It is noted that the far field of the magnetic dipole is $90^\circ$ out of time phase with the electric dipole, when the source currents are in phase.

As for the electric dipole, the polarization patterns for magnetic dipole axes oriented in the x and y directions could be deduced from the derived loci on the surface on the sphere. For the dipole axis oriented in the x direction the pattern would be that of Fig. 14(a) rotated by $90^\circ$, (u, v) axes fixed. For the dipole oriented in the y direction, the pattern will be that of Fig. 14(b).

Magnetic Dipole:

$$_z E = \frac{\omega\mu Ia^2 k \ \sin\theta \ \underline{\varphi}_0}{4\pi r} \tag{52}$$

$$_x E = \frac{-\omega\mu Ia^2 k \ (\sin\varphi \ \underline{\theta}_0 \ + \ \cos\theta\cos\varphi \ \underline{\varphi}_0)}{4\pi r} \tag{53}$$

$$_y E = \frac{\omega\mu Ia^2 k \ (\cos\varphi \ \underline{\theta}_0 \ - \ \cos\theta\sin\varphi \ \underline{\varphi}_0)}{4\pi r} \tag{54}$$

The above equations can be derived directly from the duality between the electric and magnetic dipoles (Ref. 14).

cry
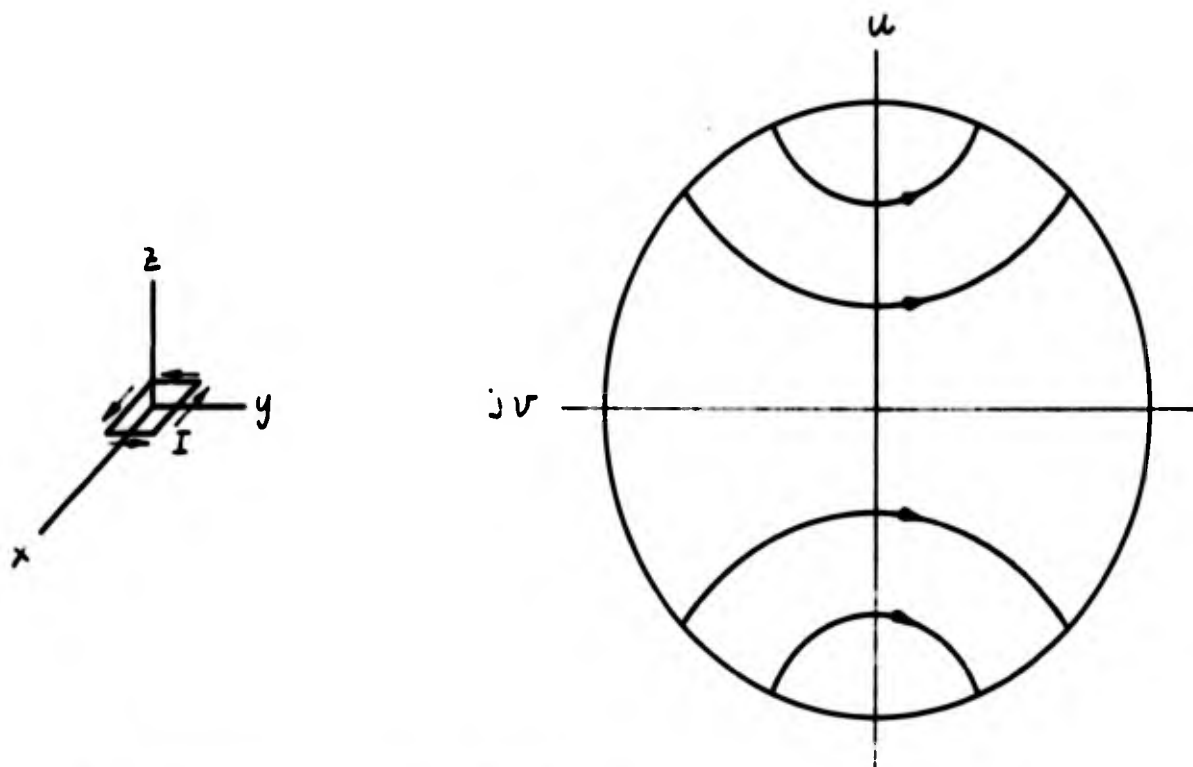
(a) Magnetic dipole - axis in z direction.
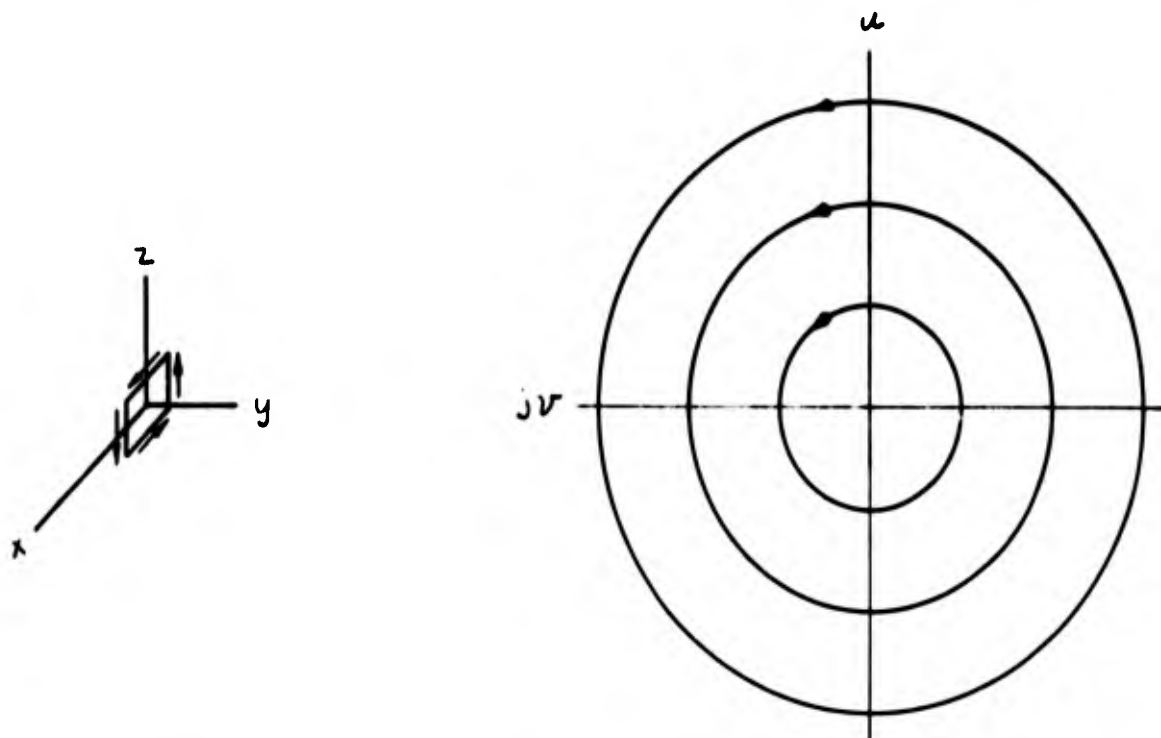


(b) Magnetic dipole - axis in y direction.

Fig. 14 - Linear polarization patterns of magnetic dipole.

The Huygens source is one of the fundamental sources in electromangetic theory. It is an orthogonal electric and magnetic field in phase and acting at a point in free space. This source is used as a tool in computing far fields from the integration of the aperture fields of waveguides, horns, reflectors etc (Ref. 17). Because of its usefulness, the polarization patterns of the Huygens source is of practical importance as well as academic interest.

The Huygens source can also be thought of as consisting of an electric and magentic dipole, oriented as shown in Fig. 15(a), with source currents in phase quadrature (Ref. 14). It will be considered in this way so that the fundamental current element may be used for the analysis. The far electric fields of the electric and magnetic dipole are added in terms of spherical coordinates.

$$E_e + E_m = \frac{j\omega\mu I_1 a \sin\theta \ \underline{\theta}_0}{4\pi r} - \frac{\omega\mu I_2 a^2 k \ (\sin\varphi \, \underline{\theta}_0 + \cos\theta \cos\varphi \ \underline{\varphi}_0)}{4\pi r} \quad (55)$$

$$I_1 = |I_1| \ \underline{/0^0} \ \text{and} \ I_2 = -|I_2| \ \underline{/90^0} \ ; \quad |I_1| = ak|I_2| = |I| \quad (56)$$

$$B = \frac{-j\omega\mu a |I|}{4\pi r} \left[ \underbrace{(\sin\theta + \sin\varphi)}_{A} \ \underline{\theta}_0 + \underbrace{\cos\theta \cos\varphi}_{B} \ \underline{\varphi}_0 \right] \quad (57)$$

In appendix III the same formula is derived for orthogonal and in phase electric and magnetic fields (the true Huygens source).

The mapping of the polarization pattern to the complex plane is accomplished by formulas (46) and (47). Omitting constants, the following results are obtained.

$$E_u = -(\sin\theta + \sin\varphi) \ \frac{\sin\theta + \sin\varphi}{1 + \sin\theta \sin\varphi} - \cos\theta\cos\varphi \ \frac{\cos\theta\cos\varphi}{1 + \sin\theta \sin\varphi}$$

$$E_v = (\sin\theta + \sin\varphi) \ \frac{\cos\theta\cos\varphi}{1 + \sin\theta \sin\varphi} - \cos\theta\cos\varphi \ \frac{\sin\theta\sin\varphi}{1 + \sin\theta \sin\varphi}$$

$$E_u = -(1 + \sin\varphi \sin\theta) \quad (60)$$

$$E_v = 0 \quad (61)$$

cry
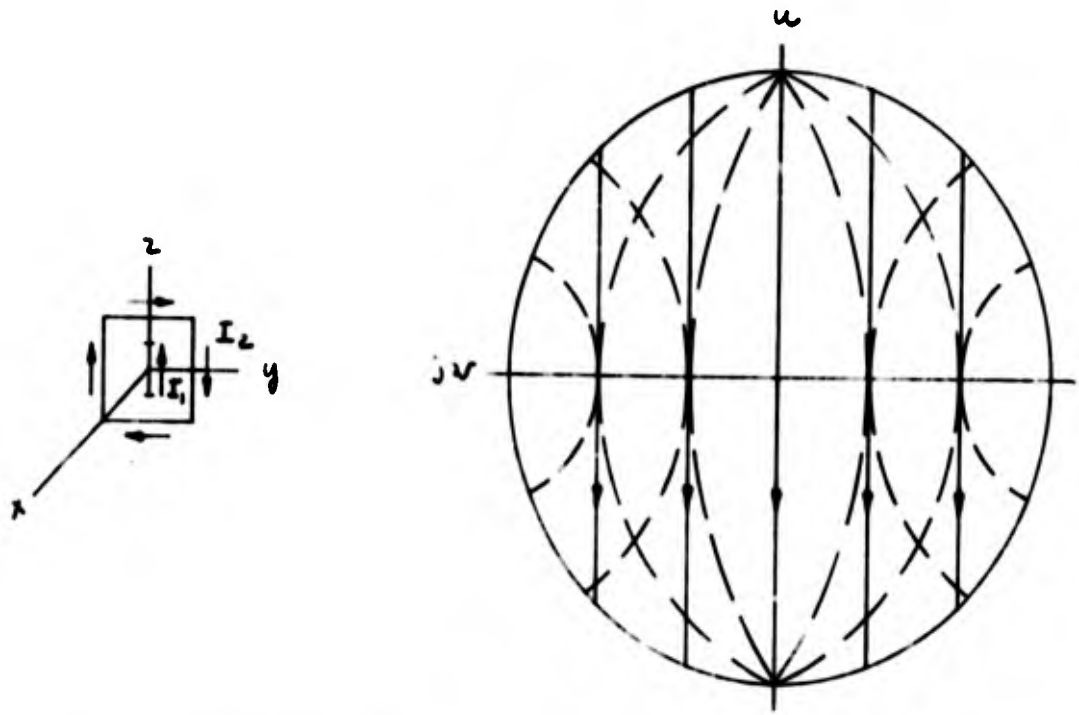
(a)  Huygens source - parallel to y z plane.
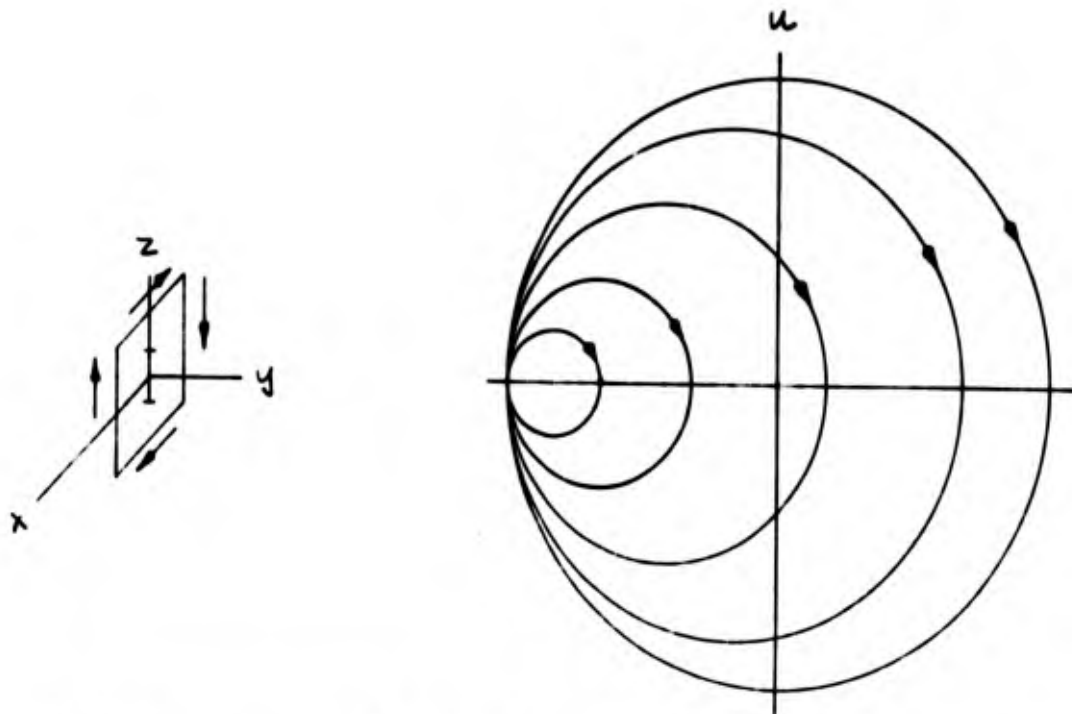


(b)  Huygens source - parallel to xz plane.

Fig. 15 - Linear polarization patterns of Huygens source.

The polarization pattern of each antenna is shown dashed in Fig. 15(a). The resultant polarization pattern is a family of straight lines all oriented parallel to the $\underline{v}_o$ direction. This can be considered an ideal result, since this source is sometimes referred to as plane wave source and what could be more plane that a family of straight lines (Ref. 3). The polarization patterns for orientations of the two dipoles parallel to the x,z plane is shown in Fig. 14(b); the pattern for orientation in the x,y plane can easily be deduced.

Another interesting polarization pattern computed was that of an electric and magnetic dipole whose axes were aligned and whose currents were in phase quadrature. The polarization pattern is a family of loxodromes (rhumb lines) on the radiation sphere (Ref. 2).

An array of electric and magnetic dipoles can be combined to produce any non-isotropic polarization pattern by variations in the magnitude, phase and orientation of their currents.

Using the electric dipole current element as a fundamental building block of antennas the far field polarization pattern of the electric dipole, magnetic dipole, Huygens source and loxodromic source were derived. The analytic mapping of the polarization was accomplished using the formulas derived in previous sections. The value of this method of analysis will be demonstrated further in the Sections VI and VII where circular and elliptical polarization patterns are computed.

cry

## VI.  Mapping of the Circular Polarization Patterns of Antennas.

A circular polarization pattern occurs when for each direction from the antenna the wave polarization is circular; the polarized wave can then be considered to result from two orthogonal linearly polarized waves of equal amplitude, but $90^{\circ}$ out of time phase.  The circular polarization patterns of the E and M dipole and crossed Huygens sources have been computed and mapped on the complex plane.

The E and M dipole is comprised of an electric dipole whose axis is coincident with the axis of a magnetic dipole, as shown in Fig. 16.  The currents of the dipoles are in phase, but of unequal amplitude.  The equations for the far electric field which have been derived previously are listed below.

$$E_e = \frac{j\omega\mu I_1 a \sin \theta \, \underline{\theta}_0}{4\pi r} \tag{62}$$

$$E_m = \frac{-\omega\mu I_2 a^2 \sin \theta \, \underline{\varphi}_0}{4\pi r} \tag{63}$$

From the above equations $E_e$ and $E_m$ are orthogonal and $90^{\circ}$ out of phase for all $\theta$ and $\varphi$.  When the ratio $I_1/I_2 = ak$, the amplitudes will also be equal and circular polarization of a left handed sense will occur for the entire sphere.  The circular polarization pattern including gain ($|E|$ field variation) is shown in Fig. 16 with the linear polarization patterns of each dipole superimposed,  Along the great circles the amplitude will vary as the sin $\theta$; amplitude variation over the sphere for any received polarization will be that of the familiar donut.

The crossed Huygens sources consist of two sets of crossed electric and magnetic fields; each set $90^{\circ}$ out of time phase with the other.  The same effect can be obtained by sets of electric and magnetic dipoles as shown in Fig. 17.  The resultant linear polarization patterns are shown in Fig. 17; the corresponding formulas for the electric fields are listed below and the derivations can be found in Section IV and in Appendix III.

cry
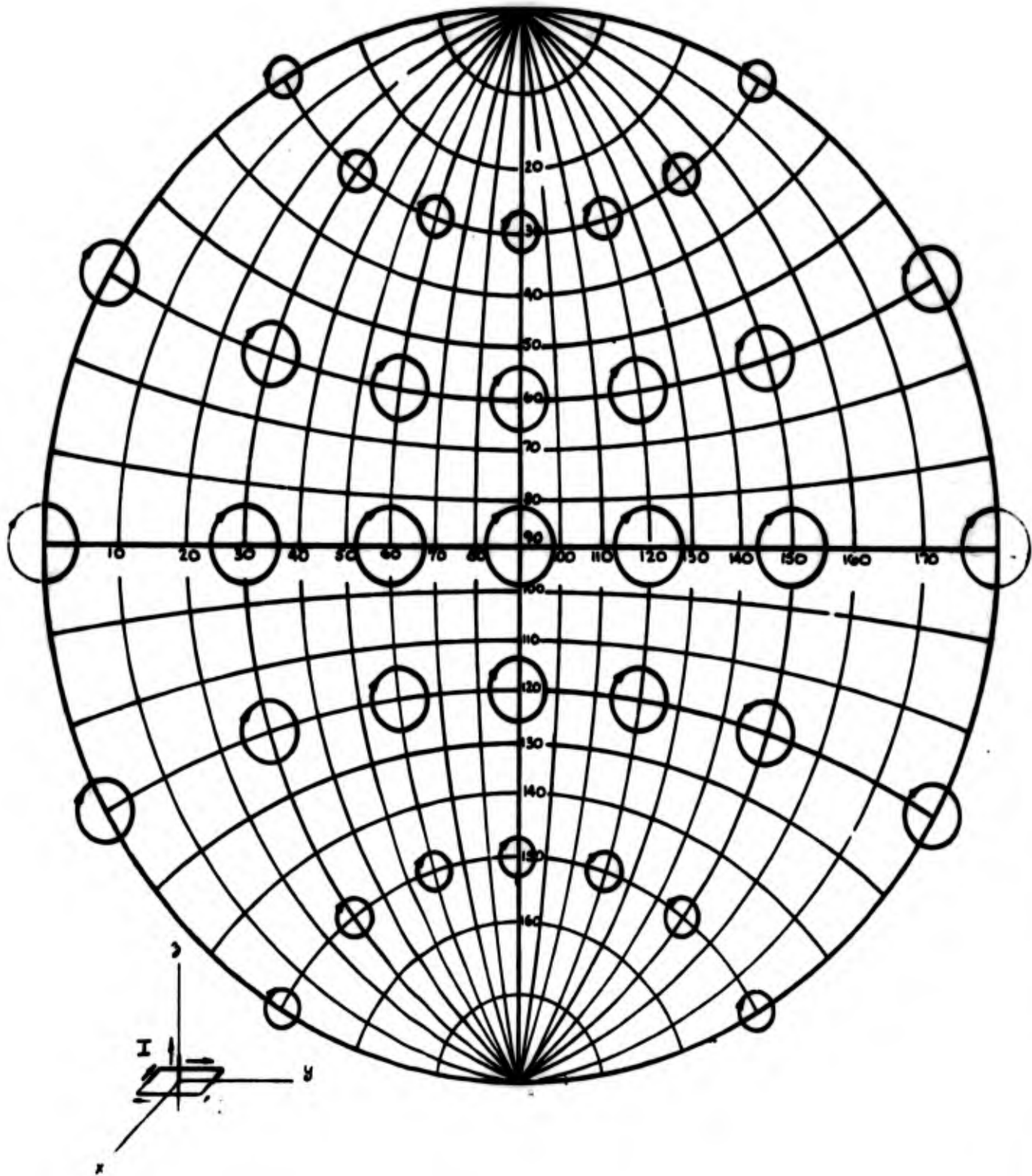
Fig. 16 - Polarization pattern of a combined electric and magnetic dipole.

$$E_u = (1 + \sin \theta \sin \varphi) \tag{64}$$

$$E_v = j(1 + \sin \theta \sin \varphi) \tag{65}$$

Since the expressions for $E_u$ and $E_v$ are identical and $30^{\circ}$ out of time **and space phase** for all points on the radiation sphere, a circular polarization pattern results. The sense is left handed and the pattern including gain for the forward hemisphere is shown in Fig. 17; the amplitude variation over the sphere for any polarization will be that of a cardioid of revolution.

cry

Fig. 17 - Polarization pattern of crossed Huygens sources.

# VII. Mapping of Elliptical Polarization Patterns of Antennas.

The methods for computing and mapping the elliptical polarization patterns of antennas are outlined. The polarization pattern of the turnstile antenna has been computed and mapped on the complex plane.

The turnstile antenna is made up of crossed electric dipoles $I_z$ and $I_x$ whose source currents are of equal magnitude, but $90^o$ out of time phase. The mapped far field linear polarization pattern of each radiator is shown superimposed in Fig. 18. It is observed from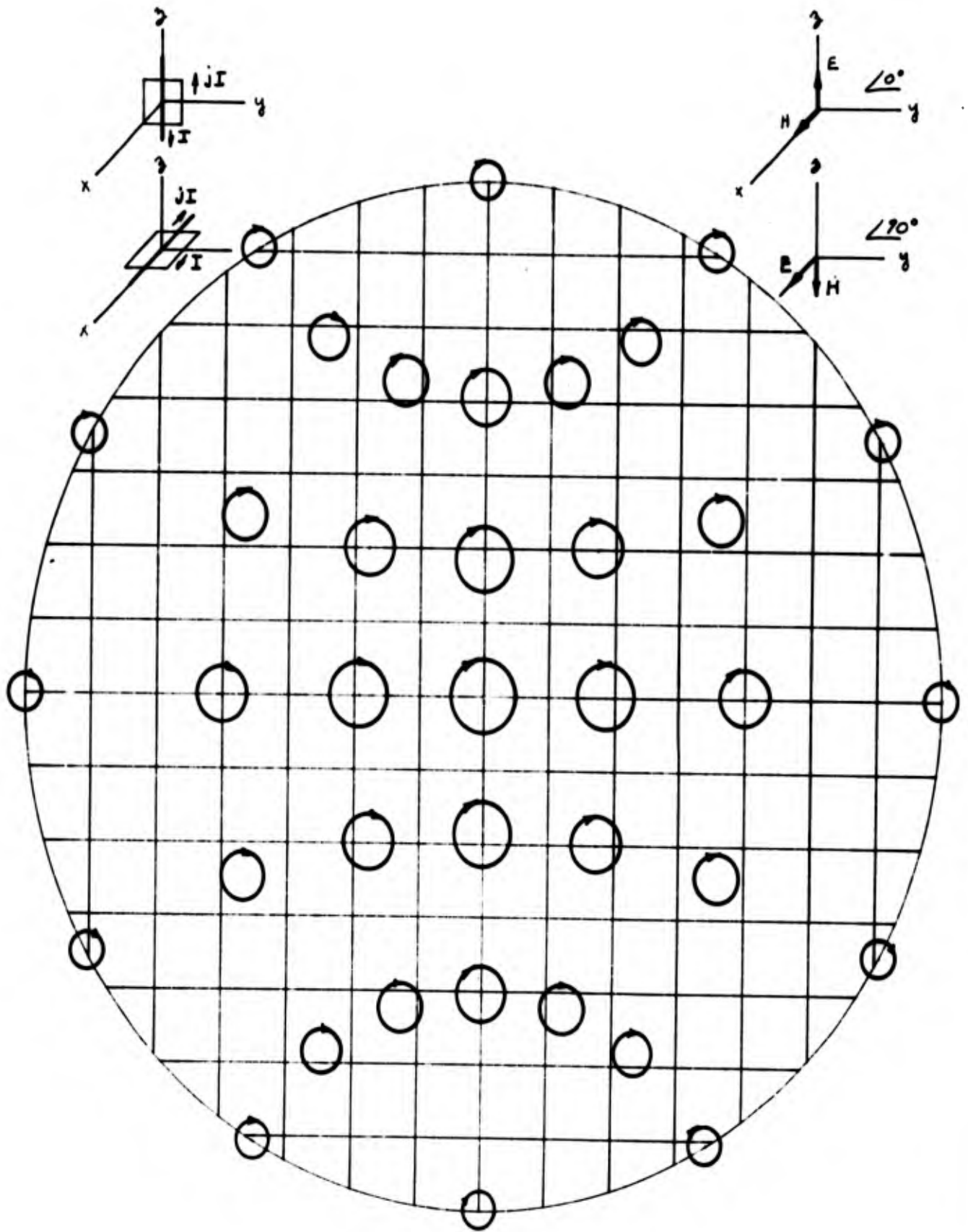 Fig. 18 that the space angle between the electric field components of each dipole changes over the sphere. In order to compute the polarization pattern it is necessary to add the $\theta_o$ and $\varphi_o$ components of each dipole and then separate these vectors into $u_o$ and $v_o$ components. In this manner there will exist two orthogonal linearly polarized waves of arbitrary amplitude and time phase referenced to the $u_o$ direction at each point on the radiation sphere, from which the polarization ellipse may be computed. This procedure is outlined in the following derivation starting with the previously derived far electric fields associated with each dipole.

$$_xE = J(\cos \theta \cos \varphi\, \theta_o - \sin \varphi \varphi_o) \tag{66}$$

$$_zE = - \sin \theta\, \theta_o \tag{67}$$

$$_xE + {}_zE = \underbrace{- J \sin \varphi}_{B}\, \varphi_o + \underbrace{(J \cos \theta \cos \varphi - \sin \theta)}_{A}\, \theta_o \tag{68}$$

$$E_u = - A \cos \sigma - B \sin \sigma \tag{69}$$

$$E_v = A \sin \sigma - B \cos \sigma \tag{70}$$

$$E_u = -(- \sin \theta + J \cos \theta \cos \varphi)\cos \sigma -(- J \sin \varphi)\sin \sigma \tag{71}$$

$$E_v = (- \sin \theta + J \cos \theta \cos \varphi)\sin \sigma -(- J \sin \varphi)\cos \sigma \tag{72}$$

cry
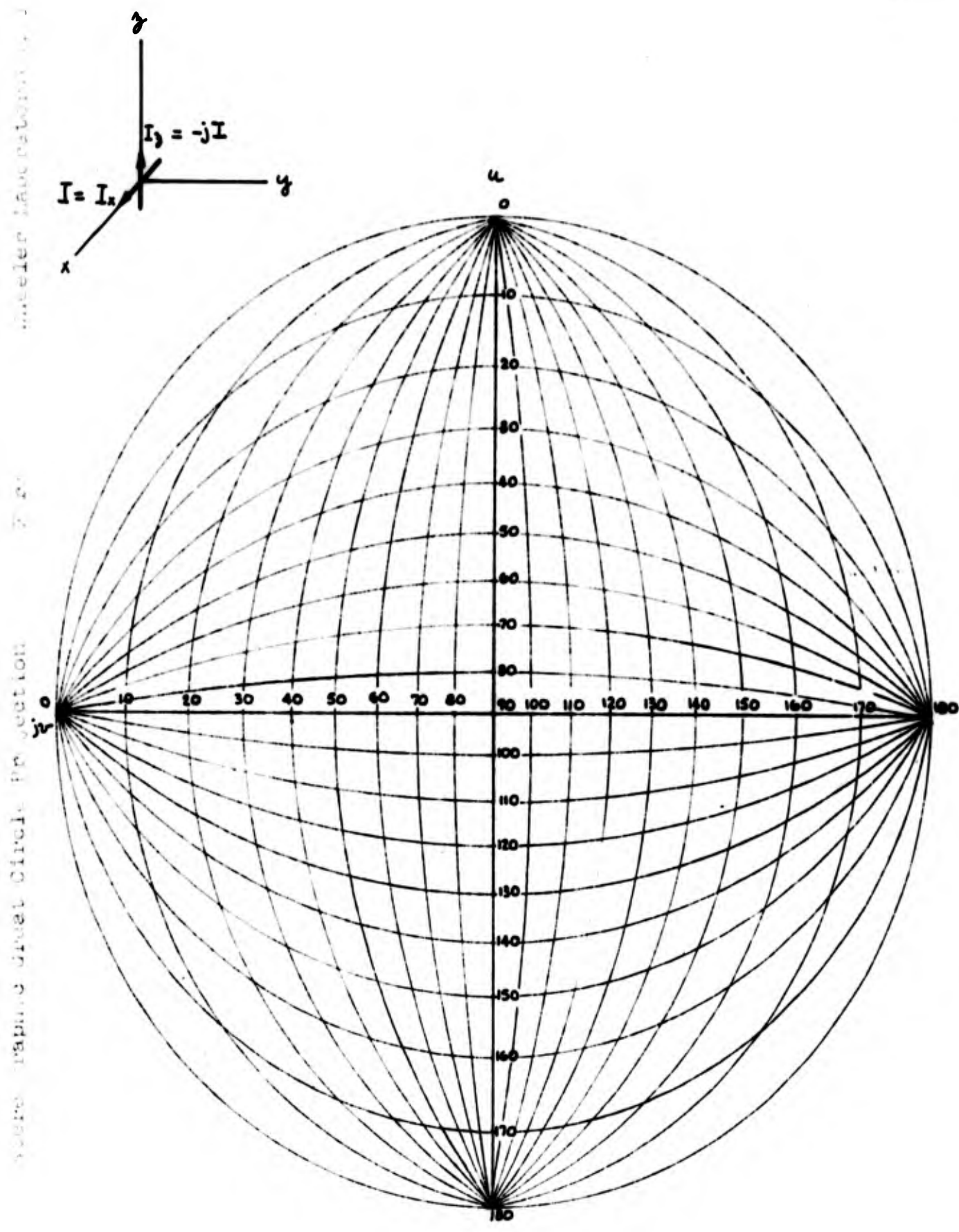
Fig. 18 - Linear polarization patterns of turnstile antenna elements.

$$E_u = \sin\theta\cos\sigma + j(\sin\varphi\sin\sigma - \cos\theta\cos\varphi\cos\sigma) \quad (73)$$

$$E_v = -\sin\theta\sin\sigma + j(\sin\varphi\cos\sigma + \cos\theta\cos\varphi\sin\sigma) \quad (74)$$

$$E_u = u_a + j\,u_b = \sqrt{u_a^2 + u_b^2}\ \tan^{-1} u_b/u_a \quad (75)$$

$$E_v = v_a + j\,v_b = \sqrt{v_a^2 + v_b^2}\ \tan^{-1} v_b/v_a \quad (76)$$

$$u_a = \sin\theta\cos\sigma \quad (77)$$

$$u_b = (\sin\varphi\sin\sigma - \cos\theta\cos\sigma\cos\sigma) = -\sin\theta\sin\sigma \quad (78)$$

$$v_a = -\sin\theta\sin\sigma = u_b \quad (79)$$

$$v_b = \sin\varphi\cos\sigma + \cos\theta\cos\varphi\sin\sigma \quad (80)$$

The amplitude and phase of the $E_u$ and $E_v$ field components have been computed as a function of $\theta$ and $\varphi$ and are tabulated in Table I. From these field components the axial ratio, tilt angle, sense and maximum amplitude have been computed using the wave polarization chart and relationships described in Section III, the results are listed in Table I. A sample calculation of the axial ratio, tilt angle and sense for $\theta = \varphi = 30°$ has been outlined in Section III. From the table the elliptical polarization pattern is mapped on the complex plane, as shown in Fig. 19.

Some very interesting general results concerning the turnstile antenna have been derived in Appendix IV. First, the normalized maximum amplitude ($G$) is always equal to unity. Second, the absolute value of the left to right circularly polarized components

$$|q| = \frac{|L|}{|R|} = \frac{1 + \sin\theta\sin\varphi}{1 - \sin\theta\sin\varphi} \quad (81)$$

cry

cry

| SPACE ANGLES | | REAL AND IMAGINARY ELECTRIC FIELD COMPONENTS | | | ELECTRIC FIELD COMPONENTS | | AMPLITUDE RATIO | | TIME PHASE | AXIAL RATIO | | TILT ANGLE | SENSE |
|---|---|---|---|---|---|---|---|---|---|---|---|---|---|
| $\phi$ | $\theta$ | $u_a$ | $v_a$ / $u_b$ | $v_b$ | $E_u$ | $E_v$ | $\frac{E_v}{E_u}$ | db $\frac{E_v}{E_u}$ | $\delta$ | r | dbr | $\tau$ | S |
| 0 | 0 | 0 | 0 | 1.000 | 0 | $1/90$ | ∞ | ∞ | 90 | ∞ | ∞ | 90 | – |
| 0 | 30 | .250 | -.433 | .750 | $.500/\underline{-60}$ | $.865/\underline{120}$ | 1.73 | +4.73 | 180 | ∞ | ∞ | 120 | – |
| 0 | 60 | .750 | -.433 | .250 | $.865/\underline{-30}$ | $.500/\underline{150}$ | .58 | -4.73 | 180 | ∞ | ∞ | 150 | – |
| 0 | 90 | 1.000 | 0 | 0 | $1/\underline{0}$ | 0 | 0 | - | 0 | ∞ | ∞ | 0 | – |
| 30 | 30 | .400 | -.300 | .850 | $.500/\underline{-36.8}$ | $.900/\underline{109.4}$ | 1.80 | +5.10 | 146.2 | 4.00 | 12.0 | 116.5 | L |
| 30 | 60 | .825 | -.261 | .606 | $.864/\underline{-17.6}$ | $.660/\underline{113.4}$ | .76 | -2.35 | 131 | 2.38 | 7.5 | 146.5 | L |
| 30 | 90 | 1.000 | 0 | .500 | $1/\underline{0}$ | $.500/\underline{90}$ | .50 | -6.00 | 90 | 2.00 | 6.0 | 0 | L |
| 60 | 30 | .476 | +.151 | .955 | $.500/\underline{-17.6}$ | $.968/\underline{99}$ | 1.93 | +5.70 | 116.6 | 2.30 | 7.2 | 106.5 | L |
| 60 | 60 | .856 | -.123 | .890 | $.867/\underline{-8.2}$ | $.900/\underline{97.5}$ | 1.04 | + .35 | 105.7 | 1.37 | 2.3 | 131.5 | L |
| 60 | 90 | 1.000 | 0 | .866 | $1/\underline{0}$ | $.866/\underline{30}$ | .87 | + .94 | 30 | 1.15 | .3 | 0 | L |
| 90 | 30 | .500 | 0 | 1.000 | $.500/\underline{0}$ | $1/\underline{90}$ | 2.00 | +6.00 | 30 | 2.00 | 6.0 | 90 | L |
| 90 | 60 | .866 | 0 | 1.000 | $.866/\underline{0}$ | $1/\underline{90}$ | 1.15 | + .94 | 30 | 1.15 | .9 | 30 | L |
| 90 | 90 | 1.000 | 0 | 1.000 | $1/\underline{0}$ | $1/\underline{90}$ | 1.00 | 0 | 30 | 1.00 | 0 | -- | L |

Table I - Turnstile antenna elliptical polarization pattern data.
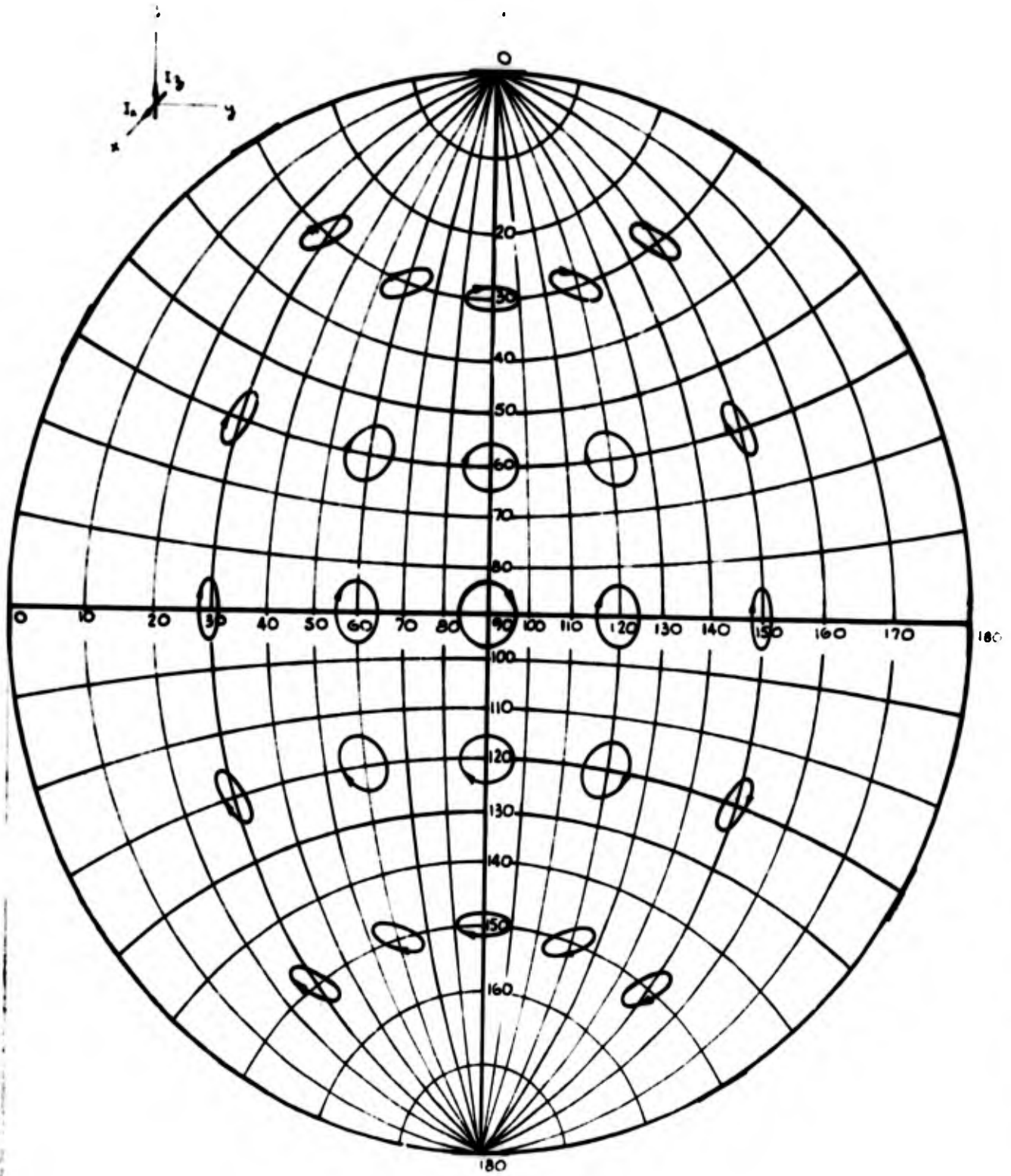
Fig. 19 - Polarization pattern of turnstile antenna.

Third, the tilt angle ($\tau$) of the major axis with respect to the $\underline{u}_0$ direction is equal to

$$\tau = \tan^{-1}(-\tan \theta \cos \varphi) \tag{82}$$

this corresponds to the direction ($\frac{du}{dv}$) tangent to concentric circles about the cneter of the complex plane. Fourth, the axial ratio (r) is equal to

$$r = \frac{1}{1 + \sin \theta \sin \varphi} \tag{83}$$

Fifth, the constant power gain contours are concentric with the origin; the power density (S) varying as

$$S = \frac{1 + r^2}{r^2} \tag{84}$$

(Ref. 16). Lastly, the polarization pattern includes all possible wave polarizations. The turnstile antenna is an excellent instructive example of antenna and wave polarization.

cry

## VIII.  Computation of the Polarization Loss of Two Elliptically Polarized Antennas.

In transmit-receive systems, the loss of signal as a result of polarization mismatch is of interest.  The geometry of this type of system is shown in Fig. 20.  The transmitting and receiving antennas, for example, are turnstile antennas whose axes are oriented as shown.  The transmitting antenna is assumed to be fixed with the receiving antenna having a variable orientation given by the angle $(e)$.

Since the elliptical polarization pattern of each antenna is known, the amount of power transferred from the transmit antenna to the other in terms of the geometry can be determined by an analysis using the stereographic projection of the receive radiation sphere (Ref. 19).  The formula for the loss of signal as a function of the type of polarization of each antenna and orientation of the polarization ellipses is given below and can be derived from the power transfer considerations between the two antennas (Ref. 4 and 3).

$$\frac{P}{Po} = \frac{1}{2}\left[1 \pm \frac{4rr' + (r^2 - 1)\ (r'^2 - 1)\ \cos 2\upsilon}{(r^2 + 1)\ (r'^2 + 1)}\right] \qquad (85)$$

The necessary information are the axial ratios $r$ and $r'$, the sense of rotation, same or opposite (+ and - respectively) and the angular separation $(\upsilon)$ between the two major axes of the polarization ellipses.

Given the separation of unity and the direction from the transmit antenna to the receiving antenna in terms of $\theta$ and $\varphi$, then the direction from the receive antenna to the transmit antenna in terms of $\theta'$ and $\varphi'$ may be found.  The properties of both wave polarization ellipses are then known.  It remains to compute the angular separation.

A description of the analysis to find the angular separation $(\upsilon)$ using the complex plane is given below.  The basic principle of this method is to refer to the transmit wave polarization tilt angle $(\tau)$ to the $\underline{u}_o$ direction and the receive wave polarization tilt angle $(\tau')$ to the $\underline{u}'_o$ direction and then
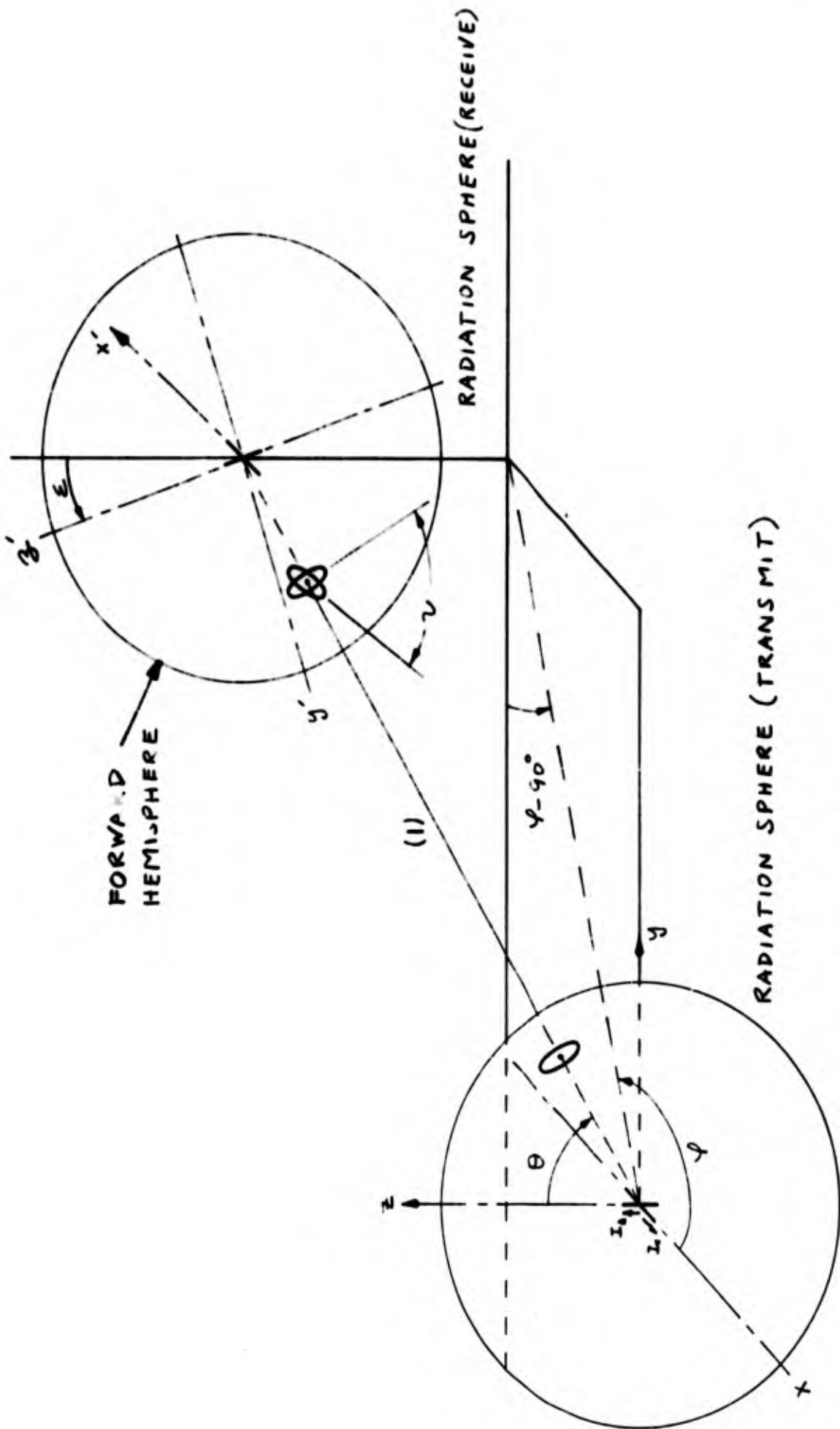
cry

Fig. 20 - Geometry of transmit - receive antenna system.
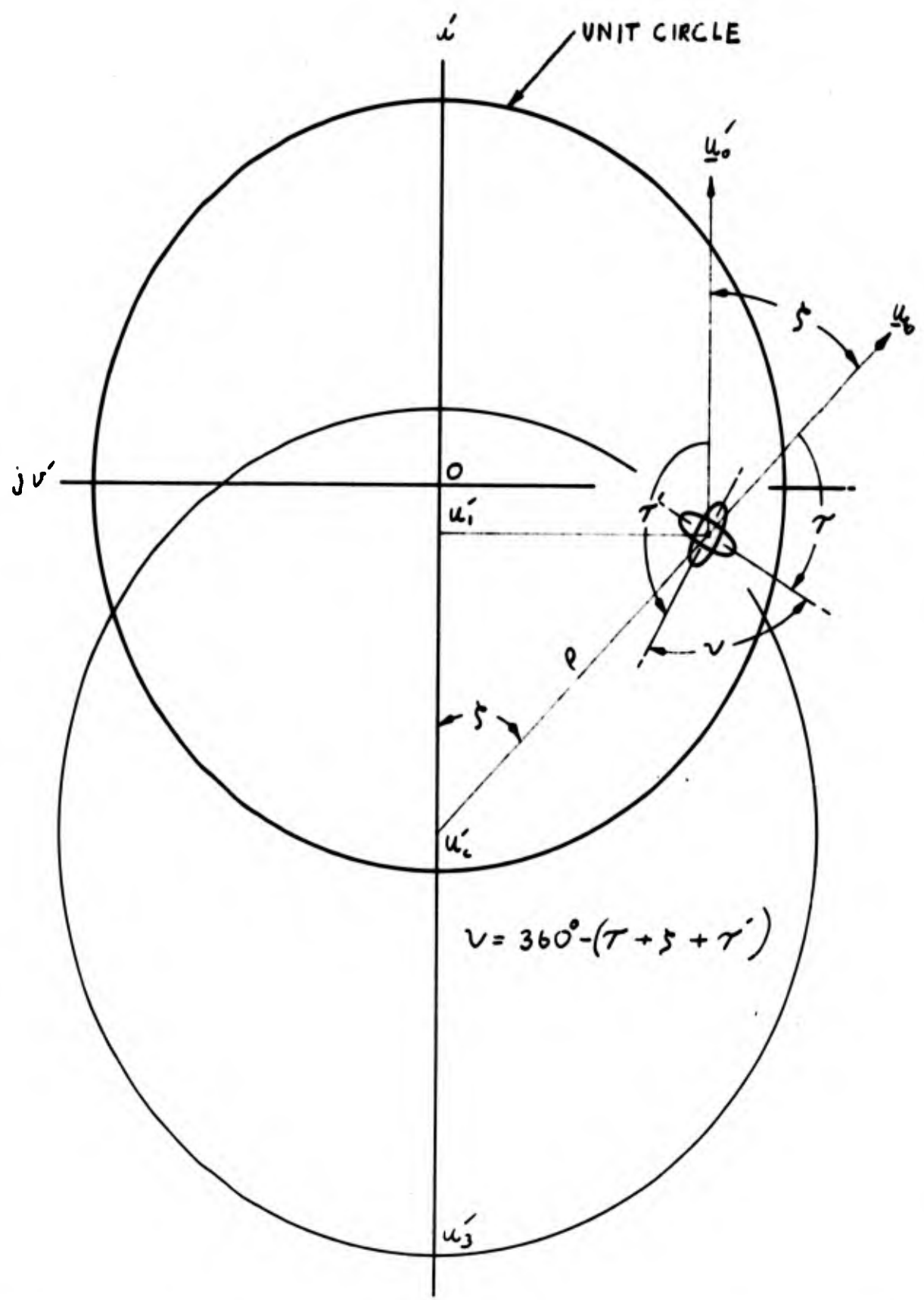
Fig. 21 - Derivation of angular separation (υ) on complex plane. of receive forward hemisphere.

conformally transform the $u_0$ direction to the receive sphere. The resultant diagram on the complex plane is shown in Fig. 21. The angular separation $\upsilon$ equals $360 - (\tau + \zeta + \tau')$ where $(\zeta)$ is the angle between the $u_0$ and $u_{0'}$ directions. The figures and formulas describing the transformation and derivation of $(\zeta)$ are included in Appendix V for reference. Since they are complicated and difficult to explain, they have b'en omitted from the body of the thesis and no attempt is made to explain them in the appendix.

cry

## IX. References.

(1)  E. J. Townsend, "Functions of a Complex Variable", Henry Holt and Co.; 1915.  (Stereographic projection; mathematical transformations and proof of conformality, p. 184-189.)

(2)  C. H. Deetz and O. S. Adams, "Elements of Map Projection", U. S. Govt. Printing Office; 1945.  (Construction of stereographic maps; p. 37-38, 157-160.)

(3)  C. C. Cutler, "Parabolic Antenna Design for Microwaves", Proc. IRE, vol. 35, p. 1284-1294; November 1347.  (Polarization Pattern of plane wave source.)

(4)  Sichak, and Milazzo, "Antennas for Circular Polarization", Proc. IRE vol. 36, p. 997; August 1948.  (Derivation of polarization loss formula based on linearly polarized components of elliptically polarized waves.)

(5)  H. A. Wheeler, "Geometric Relations in Circle Diagrams of Transmission Line Impedance", Wheeler Monographs, Vol. I, No. 4; 1948.  (Two-fold stereographic projection, coordinate conventions.)

(6)  E. A. Guillemin, "The Mathematics of Circuit Analysis", John Wiley and Sons; 1949.  (Definitions of conformal and isogonal; mapping of sphere to plane and sphere to sphere, p. 253-263, 360-378.)

(7)  L. A. Ware, "Elements of Electromagnetic Waves", Pitman Publishing Corp., 1949.  (Electromagnetic radiation; theoretical discussion, p. 181-200.)

(8)  Sinclair, "Elliptically Polarized Waves", Proc. IRE, p. 148; Feb. 1950.

(9)  Hatkin, "Elliptically Polarized Waves", Proc. IRE Corresp. p. 997; Dec. 1350.  (Derivation of polarization loss formula based in circularly polarized components of elliptically polarized waves.)

cry

(10)  J. D. Kraus, "Antennas", McGraw Hill; 1950.  (Fundamentals of wave polarization, p. 464-484.)

(11)  Booker, Rumsey, Deschamps, Bonnert, "Techniques for Handling Elliptically Polarized Waves", Proc. IRE, p. 533, May 1951. (Polarization chart; properties of wave polarization.)

(12)  G. C. Authenreith, "Elements of Descriptive Geometry", CCNY School of Technology; 1951.  (Descriptive techniques for geometric problems.)

(13)  D. D. King, "Measurements at Centimeter Wavelengths", D. Van Nostrand; 1952.  (Wave polarization formulas charts, p. 298-309.)

(14)  S. A. Schelkunoff and H. T. Friis, "Antenna Theory and Practice",  Wiley and Sons Inc.; 1952.  (Field equivalence theorm, electric and magnetic current sources, p. 515-522.)

(15)  G. A. Deschamp "A Hyperbolic Protractor for Microwave Impedance Measurements and Other Purposes, "Federal Telecommunications Laboratories; 1953.  (Polarization chart; novel solutions to polarization problems using hyperbolic protractor, p. 31-35.)

(16)  J. D. Kraus, "Electromagnetics", McGraw Hill; 1953 (Power in Elliptically polarized field, p. 379-387.)

(17)  E. M. T. Jones, "Paraboloid Reflector and Hyperboloid Lens Antennas", PGAP, p. 119; July 1954.  (Field in aperture of reflectors and lenses, Huygens source best.)

(18)  D. M. Y. Sommerville, "The Elements of Non-Euclidean Geometry", Dover Publications; 1959.  (Stereographic projection, p. 172.)

(19)  J. D. Hanfling, "Formulas for Direction and Polarization of a Tracking Radar as seen by a Missile Antenna".  WL Report 801, to BTL; Mar. 1960.  (Application of stereographic projection to polarization problems.)

cry

## Appendix I:  Polarization Ellipse Deviation.

$$E = E_u + E_v \tag{1}$$

$$E = E_R + E_L \tag{2}$$

$$E_R = R(\underline{u}_o - J\underline{v}_o) \tag{3}$$

$$E_L = L(\underline{u}_o + J\underline{v}_o) \tag{4}$$

$$E_u = L + R, \qquad L = \frac{E_u - JE_v}{2} \tag{5}$$
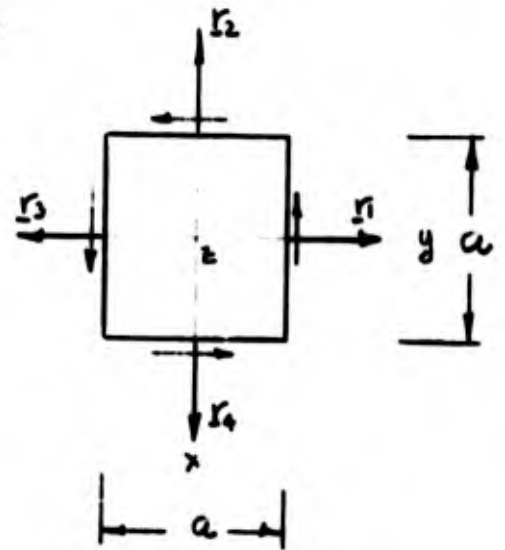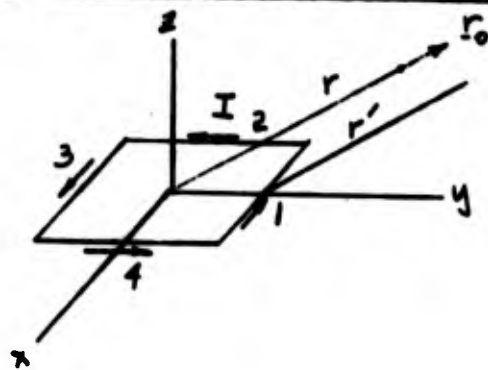
$$E_v = J(L - R), \qquad R = \frac{E_u + JE_v}{2} \tag{6}$$

$$\frac{E_v}{E_u} = P = J\left(\frac{L - R}{L + R}\right) = J\frac{\frac{L}{R} - 1}{\frac{L}{R} + 1}, \qquad \frac{L}{R} = q \tag{7}$$

$$P = JF = \frac{1 - q}{1 + q} \tag{8}$$

$$q = \frac{1 - p}{1 + p} \tag{9}$$

$$r = \frac{1 + |q|}{1 - |q|} \quad \text{for } |q| > 1 \tag{10}$$

cry

## Appendix II: The Magnetic Dipole.



General far field equation:

$$E = \frac{-j\omega\mu\Delta l}{4\pi r} \left[ (\underline{I} \cdot \underline{\theta}_o) \ \underline{\theta}_o + (\underline{I} \cdot \underline{\varphi}_o) \ \underline{\varphi}_o \right] \exp -jkr' \tag{11}$$

$$r' = r - (\underline{r}_n \cdot \underline{r}_o) \tag{12}$$

$$\underline{r}_1 = \frac{a}{2} \underline{y}_o, \qquad r_2 = -\frac{a}{2} \underline{x}_o \tag{13}$$

$$r_3 = -\frac{a}{2} \underline{y}_o, \qquad r_4 = \frac{a}{2} \underline{x}_o \tag{14}$$

$$(\underline{I} \cdot \underline{\theta}_o) \ \underline{\theta}_o + (\underline{I} \cdot \underline{\varphi}_o) \ \underline{\varphi}_o = \underline{I} \cdot \underbrace{(\underline{\theta}_o \ \underline{\theta}_o + \underline{\varphi}_o \ \underline{\varphi}_o)}_{\epsilon_t} = \underline{I} \cdot \epsilon_t \tag{15}$$

$$K = \frac{-j\omega\mu a I \ \exp -jkr}{4\pi r} \tag{16}$$

Treating $r_1$ and $r_3$ as an array and $r_2$ and $r_4$ as an array

$$E_1 + E_3 = K \left[ -\underline{x}_o \cdot \epsilon_t \ \exp jk(\underline{r}_1 \cdot \underline{r}_o) + \underline{x}_o \cdot \epsilon_t \ \exp jk(\underline{r}_3 \cdot \underline{r}_o) \right] \tag{17}$$

$$E_2 + E_4 = K \left[ -\underline{y}_o \cdot \epsilon_t \ \exp jk(\underline{r}_2 \cdot \underline{r}_o) + \underline{y}_o \cdot \epsilon_t \ \exp jk(\underline{r}_4 \cdot \underline{r}_o) \right] \tag{18}$$

$$\underline{x}_o \cdot \epsilon_t = \cos\theta \cos\varphi \ \underline{\theta}_o - \sin\varphi \ \underline{\varphi}_o \tag{19}$$

$$\underline{y}_o \cdot \epsilon_t = \cos\theta \sin\varphi \ \underline{\theta}_o + \cos\varphi \ \underline{\varphi}_o \tag{20}$$

cry

$$\underline{r}_1 \cdot \underline{r}_0 = \frac{a}{2}(\underline{y}_0 \cdot \underline{r}_0) = \frac{a}{2}\sin\varphi\sin\theta \tag{21}$$

$$r_4 \cdot \underline{r}_0 = \frac{a}{2}(\underline{x}_0 \cdot \underline{r}_0) = \frac{a}{2}\cos\varphi\sin\theta \tag{22}$$

$$E_1 + E_3 = -K2J(\cos\theta\cos\varphi\,\underline{\theta}_0 - \sin\varphi\,\underline{\varphi}_0)\left[\sin(\frac{ka}{2}\sin\varphi\sin\theta)\right] \tag{23}$$

$$E_2 + E_4 = K2J(\cos\theta\sin\varphi\,\underline{\theta}_0 + \cos\varphi\,\underline{\varphi}_0)\left[\sin(\frac{ka}{2}\sin\theta\cos\varphi)\right] \tag{24}$$

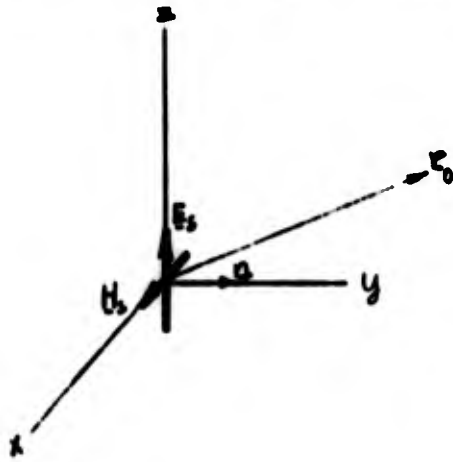$$\text{if} \quad \frac{ka}{2} = \frac{2\pi a}{\lambda 2} = \frac{a\pi}{\lambda} \tag{25}$$

$$\text{if} \quad a \leq \frac{\lambda}{4} \text{ then } \sin\alpha = \alpha \tag{26}$$

$$E_T = JKka\,\sin\theta\,[(-\sin\varphi\cos\theta\cos\varphi + \cos\theta\sin\varphi\cos\varphi\,\underline{\theta}_0 + \tag{27}$$
$$\sin^2\varphi + \cos^2\varphi)\,\underline{\varphi}_0] = JKka\,\sin\theta\,\underline{\varphi}_0$$

$$\underline{E}_T = \frac{\omega\mu\,\exp-jkr\,Ia^2k\,\sin\theta\,\underline{\varphi}_0}{4\pi r} \tag{28}$$

holds within 10% for $\left(a \leq \frac{\lambda}{4}\right)$

cry

## Appendix III:  The Hugyens Source.



For short current element

$$\underline{E}_1 = \underbrace{\frac{-j\omega\mu \ \exp \ -jkr}{4\pi r}}_{C} \ (I\Delta l \cdot \underline{e}_t) = C \ dS \ (nx\underline{H}_s \cdot \underline{e}_t) \tag{29}$$

$$\underline{I} \ \Delta l = \underline{J} \ dS = nx\underline{H}_s \cdot dS \tag{30}$$

By duality

$$\underline{H}_2 = \frac{j\omega\varepsilon \ \exp \ -jkr(\underline{m} \ \Delta l \cdot \underline{e}_t)}{4\pi r} = \frac{C \ dS}{\zeta^2} \ (nx\underline{E}_s \cdot \underline{e}_t) \tag{31}$$

$$\underline{m} \ \Delta l = \underline{M} \ dS = nx\underline{E}_\varepsilon \cdot dS \tag{32}$$

$$E_2 = (\underline{H}_2 x\underline{r}_o) \ \zeta \tag{33}$$

$$E_T = E_1 + E_2 = C \ dS\left[(nx\underline{H}_s) \cdot \underline{e}_t + \frac{\underline{E}_s x\underline{n} \cdot \underline{e}_t}{\zeta} x \underline{r}_o \right] \tag{34}$$

$$\underline{n}x\underline{H}_s = |\underline{n}x\underline{H}|(-\underline{z}_o) \tag{35}$$

$$-\underline{z}_o \cdot \underline{e}_t = \sin \theta \ \underline{\theta}_o \tag{36}$$

$$\frac{\underline{E}x\underline{n}}{\zeta} = \left|\frac{\underline{E}x\underline{n}}{\zeta}\right|(-\underline{x}_o) \tag{37}$$

$$-\underline{x}_o \cdot \underline{e}_t = -\left[\cos \theta \cos \varphi \ \underline{\theta}_o - \sin \varphi \ \underline{\varphi}_o\right] \tag{38}$$
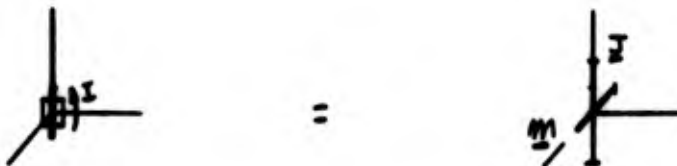
$$-\underline{x}_o \cdot \underline{e}_t x \underline{r}_o = -\left[-\cos \theta \cos \varphi \ \underline{\varphi}_o - \sin \varphi \ \underline{\theta}_o\right] \tag{39}$$

cry

$$E_T = \frac{-j\omega\mu \ \exp \ -jkr \ dS}{4\pi r} \left[ |\underline{n}x\underline{H}| \ \sin \theta \ \underline{\theta}_o + \left|\frac{Exn}{\zeta}\right| (\cos\varphi \ \cos\varphi\underline{\varphi}_o + \sin\varphi\underline{\theta}_o) \right] (40)$$

$$|\underline{n}x\underline{H}| = \frac{|Ex\underline{n}|}{\zeta} \tag{41}$$

$$E_T = \frac{-j\omega\mu \ \exp \ -jkr \ dS \ |\underline{n}x\underline{H}|}{4\pi r} \left[ (\sin\theta + \sin\varphi)\underline{\theta}_o + (\cos\theta \ \cos\varphi) \ \underline{\varphi}_o \right] (42)$$

This is the same result as obtained for an electric and magnetic dipole oriented as shown with currents 90° out of phase.



Equation (40) may be used to calculate the far field from electric and magnetic field distributions having a ratio of $E$ to $H$ other than the free space impedance.

cry

Appendix IV:  Turnstile Antenna General Results.

To Find:  Maximum Amplitude (G), $|q|$, $\tau$, r, Power Density (S)

Given:

$$E_u = u_a + ju_b \tag{43}$$

$$E_v = v_a + jv_b \tag{44}$$

See formulas (77), (78), (79), (80) Section VII,  (46), (47), Section IV , ( 5 ), ( 6) Appendix I.

To Find:  $|L| + |R| = |G|$

$$2L = u_a + ju_b - j(v_a + jv_b) = (u_a + v_b) + j(u_b - v_a) \tag{45}$$

$$2R = u_a + ju_b + j(v_a + jv_b) = (u_a - v_b) + j(u_b + v_a) \tag{46}$$

$$u_b = v_a \tag{47}$$

$$2L = u_a + v_b ; \quad 2R = u_a - v_b + j2u_b \tag{48}$$

$$2L = \sin\theta \cos\sigma + \sin\varphi \cos\sigma + \cos\theta \cos\varphi \sin\sigma \tag{49}$$

$$2L = 1 + \sin\theta \sin\varphi (\cos^2\sigma + \sin^2\sigma) \tag{50}$$

$$2L = 1 + \sin\theta \sin\varphi \tag{51}$$

$$\boxed{|L| = \frac{1 + \sin\theta \sin\varphi}{2} \underline{/0^\circ}} \tag{52}$$

$$2R = \sin\theta \cos\sigma - \sin\varphi \cos\sigma - \cos\theta \cos\varphi \sin\sigma - 2j\sin\theta \sin\sigma \tag{53}$$

$$2R = \frac{\sin^2\theta - \sin^2\varphi - \cos^2\theta \cos^2\varphi - 2j\sin\theta \cos\theta \cos\varphi}{1 + \sin\theta \sin\varphi} \tag{54}$$

$$2R = \frac{2\sin^2\theta - 1 - \sin^2\theta \sin^2\varphi - 2j\sin\theta \cos\theta \cos\varphi}{1 + \sin\theta \sin\varphi} \tag{55}$$

$$2R = \frac{1 - \sin^2\theta \sin^2\varphi}{1 + \sin\theta \sin\varphi} \underline{/\alpha} \tag{56}$$

cry

$$a = \tan^{-1} - \frac{-2\sin\theta\cos\theta\cos\varphi}{2\sin^2\theta - 1 - \sin^2\theta\sin^2\varphi} \tag{57}$$

$$\boxed{|R| = \frac{1 - \sin\theta\sin\varphi}{2} \angle a} \tag{58}$$

$$|L| + |R| = |G| = \frac{1 + \sin\theta\sin\varphi}{2} + \frac{1 - \sin\theta\sin\varphi}{2} \tag{59}$$

$$\boxed{|G| = 1} \tag{60}$$

$$|q|\exp - j2\tau = \frac{L}{R} = \frac{1 + \sin\theta\sin\varphi}{1 - \sin\theta\sin\varphi} \angle 2\tau \tag{61}$$

$$|q| = \frac{1 + \sin\theta\sin\varphi}{1 - \sin\theta\sin\varphi} \tag{62}$$

$$\tan 2\tau = + \frac{2\sin\theta\cos\theta\cos\varphi}{2\sin^2\theta - 1 - \sin^2\theta\sin^2\varphi} \tag{63}$$

$$= \frac{-2\tan\theta\cos\varphi}{\sin^2\theta - \cos^2\theta - \sin^2\theta\sin^2\varphi} \tag{64}$$

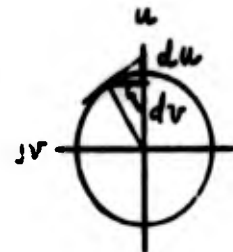$$= \frac{-2\sin\theta\cos\theta\cos\varphi}{1 - \tan^2\theta\cos^2\varphi} \tag{65}$$

$$\tan 2\tau = \frac{2\tan\tau}{1 - \tan 2\tau} \qquad \text{therefore} \tag{66}$$

$$\boxed{\tau = \tan^{-1}(-\tan\theta\cos\varphi)} \tag{67}$$

Since $u^2 + v^2 = \rho^2$ (68)

$$2u\frac{du}{dv} + 2v = 0 \tag{69}$$

$$\frac{du}{dv} = \frac{-v}{u} = -\tan\theta\cos\varphi \tag{70}$$

The major axis of the ellipse is always in the direction of the tangent to concentric circles at some $(\theta, \varphi)$

$$q > 1; \qquad r = \frac{1 + \frac{1}{|q|}}{1 - \frac{1}{|q|}} = \frac{(1 + \sin\theta\sin\varphi) + (1 - \sin\theta\sin\varphi)}{(1 + \sin\theta\sin\varphi) - (1 - \sin\theta\sin\varphi)} \tag{71}$$

$$\boxed{r = \frac{1}{\sin\theta\sin\varphi}} \tag{72}$$

cry

## Appendix V: Geometry for Computing Polarization Loss.

$$\tan \frac{\psi_u}{2} = \frac{\cos\theta}{1 + \sin\varphi \sin\theta} = u_1 \tag{73}$$

$$u_{3'} = -\cot\frac{e}{2} = -\tan\left(\frac{180 - e}{2}\right) \tag{74}$$

$$u_{2'} = \tan\left(\frac{e - \psi_u}{2}\right) \tag{75}$$

$$u_{c'} = \frac{u_{2'} + u_{3'}}{2} \tag{76}$$

$$\zeta = \sin^{-1}\frac{v_{1'}}{\rho} = \cos^{-1}\frac{u_{1'}}{\rho} \tag{77}$$

$$v_{1'} = \frac{\sin\theta' \cos\varphi'}{1 + \sin\theta' \sin\varphi'} \tag{78}$$

$$u_{1'} = \frac{\cos\theta'}{1 + \sin\varphi' \sin\theta'} \tag{79}$$

$$\rho = -u_{c'} + u_{2'} \tag{80}$$

$$v = 360^\circ - (\tau + \tau' + \zeta) \tag{81}$$

$$\tan\lambda' = \frac{\cot\theta}{\sin\varphi} \tag{82}$$

$$\sin\mu = -\sin\theta \cos\varphi \tag{83}$$

$$\cos\chi = \cos\lambda \cos\mu \tag{84}$$

$$\sin\beta = -\frac{\sin\mu}{\sin\chi} \tag{85}$$

$$\cos\gamma = \sin\theta' \sin\varphi' \tag{86}$$
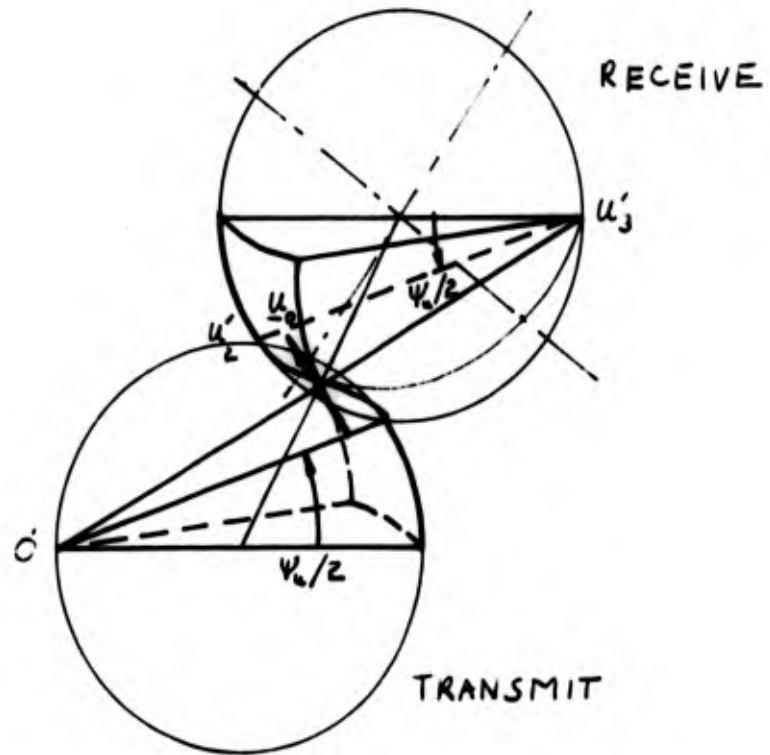
$$\cos\theta' = \frac{\cos\beta}{\sin\chi} \tag{87}$$

cry

Fig. A1 - Geometry for transformation of $\underline{u}_0$ to receive sphere.
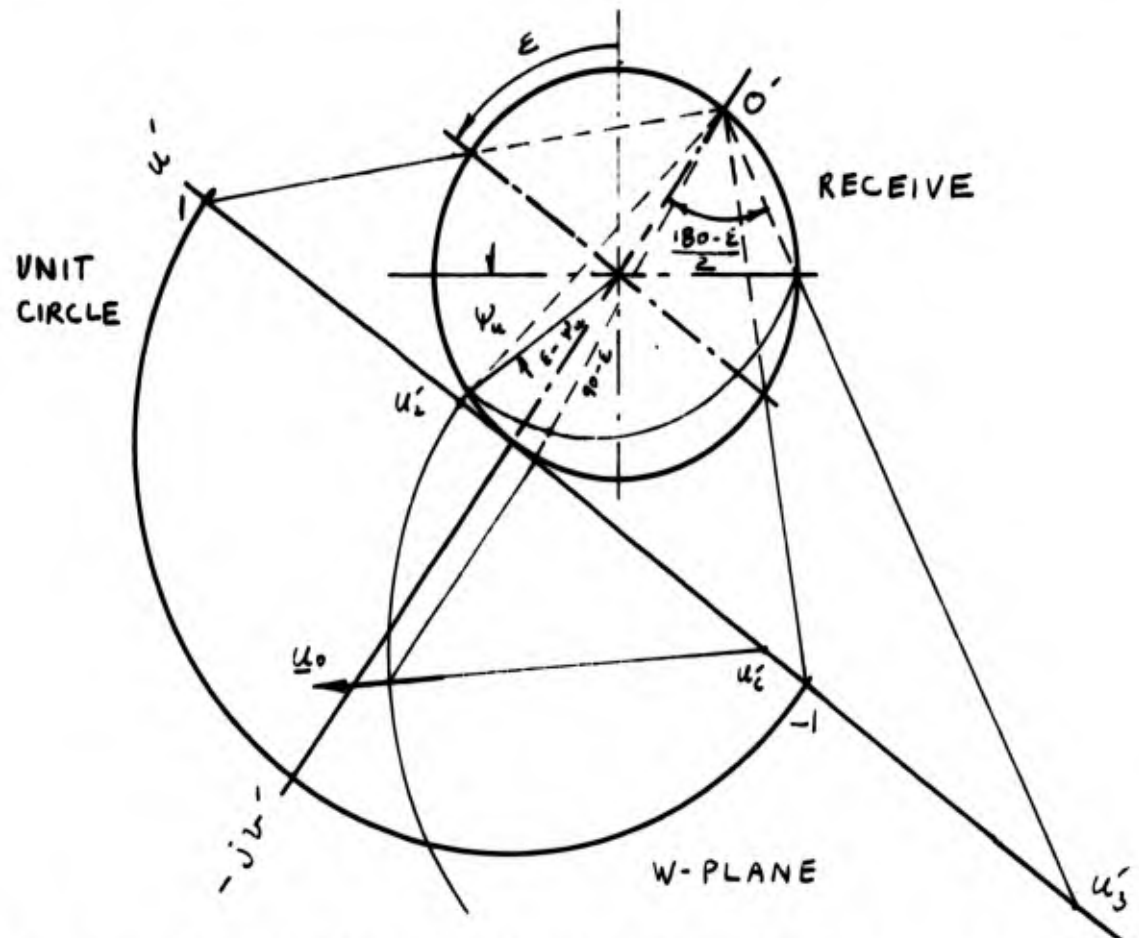


Fig. A2 - Stereographic projection of $\underline{u}_0$ to complex plane.